

1 **Observed Precipitation Associated With Air Mass**
2 **Thunderstorms over the Southern Appalachian Mountains –**
3 **28, 29 July 2008**

4
5 **Douglas K. Miller*¹, Anna M. Wilson¹, and Gregory J. Cutrell²**
6 **Ana P. Barros³ and Olivier P. Prat³**

7 ¹University of North Carolina Asheville

8 ²University of Nebraska, Lincoln

9 ³Duke University

10

11 *Journal of the Natural Hazards and Earth System Sciences*

12

13 Submitted November 2009

14 *Corresponding author:

15 Dr. Douglas K. Miller

16 UNC Asheville

17 ATMS Department, CPO#2450

18 One University Heights

19 Asheville, NC 28804

20 Email: dmiller@unca.edu

21

1 **Abstract**

2 It is well known that flood threat assessment based on low elevation gauge quantitative
3 precipitation estimates (QPEs) and radar-based QPEs in mountainous regions will lead to
4 underestimates of catchment in a single basin and a potentially false sense of security.

5 This study examines the precipitation associated with a series of ordinary (air mass)
6 thunderstorms in the southern Appalachian Mountains that occurred on 28, 29 July 2008.

7 These storms are quite common to this region during the warm season and, yet,
8 instantaneous stream flow rates after the passage of these storms increased by over five
9 times their normal amount along the Pigeon River. This particular event occurred during
10 a period of special observations consisting of an upward-looking micro-rain radar, a
11 rawinsonde system, a tethered sonde carrying fast-response temperature and moisture
12 sensors, and instruments for measuring standard meteorological surface parameters. The
13 observations were made at the center of a rain gauge network recently installed in and
14 near the Great Smoky Mountain National Park in western North Carolina.

15
16 The challenge in making QPEs in mountainous regions is that operational gauges are
17 typically located in easy-access lower elevation river valleys which lead to
18 underestimates of catchment within a river basin. Blocking of the radar beam by
19 topography compromises radar-based QPEs in mountainous regions, giving an
20 incomplete regional assessment. In general, these estimates are also compromised by
21 inhomogeneous microphysical characteristics of clouds within a single scan “snapshot”
22 and during the evolution of a precipitation event over multiple radar scan snapshots.
23 Hence, the application of a single Z-R algorithm during the passage and evolution of a
24 precipitating event can provide an inaccurate flood threat assessment.

25
26 The thunderstorms that passed over western North Carolina on 28, 29 July 2008
27 represented the dying stages of convection that had initiated over eastern Tennessee and
28 Kentucky. Rain gauge observations generally showed higher QPEs at higher elevation
29 locations. Tests of multiple Z-R algorithms applied to area NEXt Generation Weather
30 RADar (NEXRAD) radar reflectivity observations showed unimpressive correlations

1 with rain gauge observations at the location of special observations and the algorithms
2 were found generally to underestimate rainfall rates when the gauge-observed rates
3 dropped below 6 mm h^{-1} . No single algorithm gave a significantly better performance
4 among the seventeen tested. The “best” algorithms consistently underestimated the
5 accumulated precipitation for the duration of the event.

6 7 **1. Introduction**

8 Methods of making Quantitative Precipitation Estimates (QPEs) generally represent a
9 compromise between *in situ* surface-based direct point measurements or remote
10 measurements that cover a broad area (Brock and Richardson 2001). The latter method,
11 using radar and/or satellite measurements, offers potentially useful information in making
12 flooding nowcasts. The disadvantage to the remote method is that it does not directly
13 measure precipitation and so the QPE uncertainty becomes potentially large due to a
14 variety of factors. In particular, using radar-estimated reflectivity to make QPEs adds
15 uncertainty due to issues such as an unknown cloud drop size distribution, bright-band
16 effects, incomplete beam filling, and sharp gradients in rain rate (Brock and Richardson
17 2001). Accurate QPEs on short time scales are important for making accurate flood
18 forecasts and warnings and on long time scales are important for making accurate
19 assessments of the hydrological cycle.

20
21 Long-term assessments of the hydrological cycle on global scales are done almost
22 exclusively using remote (radar- and/or satellite-based) measurements. These
23 measurements are being used in climate change impact evaluations and so accurate
24 precipitation retrieval algorithms are critical in making good conclusions about the
25 effects of global warming. Geographic variations in water vapor and cloud condensation
26 nuclei sources/sinks, latitude, land surface type, and terrain elevation make global QPEs
27 challenging using remote sensing techniques. In addition, many of the direct point
28 measurement QPEs used in tuning remote precipitation retrieval algorithms for
29 mountainous regions (e.g. Himalayas) are located in valleys which tend to underestimate
30 rainfall (Barros et al. 2000).

1
2 Shorter-term assessments of the hydrological cycle on regional scales (e.g. Barros and
3 Lang 2003) generally rely on a blend of direct point and remotely measured QPEs.
4 Many studies of regional hydrological cycles have focused within the tropics due to the
5 availability of special remote measurements as part of the National Space and
6 Aeronautics Administration (NASA) Tropical Rainfall Measuring Mission (TRMM, e.g.
7 Nesbitt et al. 2004, Cecil et al. 2005). In particular, mountainous regions in the tropics
8 such as Nepal (Barros et al. 2004) and Mexico (Bhushan and Barros 2007) have received
9 much attention due to the fact that much of the population in these regions depends on the
10 mountains as a source of clean water for drinking and food production. As the emphasis
11 at NASA expands from TRMM to the Global Precipitation Measurement (GPM) mission,
12 a larger number of remote measurements of precipitation will become available for
13 studies located in regions of the mid-latitudes.

14
15 In contrast to the tropical regions, the weather and precipitation in the mid-latitudes can
16 change rather dramatically on hourly- to seasonal-time scales. The potential for rapid
17 weather change in the mid-latitudes is further complicated in mountainous regions by the
18 relative scarcity of direct meteorological measurements. As a result, operational
19 hydrological forecasting for mountainous regions in the mid-latitudes is extremely
20 challenging and individual river basins are susceptible to flash flooding without much
21 lead time when warnings are issued. Extreme hydrological events away from the
22 coastline in the eastern U.S. are often linked to the enhancement of precipitation forced
23 by mountains (Douglas and Barros 2003). A recent example of flooding and landslides
24 occurred in western North Carolina in September 2004 when the remnants of Hurricanes
25 Frances and Ivan dumped as much as 16.6” and 17.0” of rainfall, respectively, over a 24-
26 h period in the southern Appalachian Mountains (NWS 2004a, 2004b). The fluctuations
27 of weather and precipitation on short time scales in the mid-latitudes represent an
28 additional degree of complexity in making QPEs based on remote measurements.
29 One common method for making QPEs based on remote measurements involves basing
30 estimates on reflectivity measurements, the so-called Z-R relationship. Many Z-R

1 relationships have appeared in the published literature (e.g. Battan 1973 and Raghavan
2 2003) whose applications are categorized according to the type of rain event, climatic
3 region, and season of the year. The challenge in making QPEs based on the Z-R
4 relationship is that the nature of the cloud microphysics changes over the course of a
5 single precipitation event, implying a changing Z-R relationship during the evolution of a
6 single storm (Prat and Barros 2009). Current operational Z-R algorithms are unable to
7 accommodate an evolving Z-R relationship during a single precipitation event.

8 The purpose of this study is to report a detailed case study of a series of ordinary (air
9 mass) thunderstorms that occurred on 28, 29 July 2008 in the southern Appalachian
10 Mountain region at the eastern border of Tennessee and western North Carolina (Figure
11 1). The event was not extraordinary but is used to illustrate how localized embedded
12 convection in this mountainous region can cause dramatic increases in stream flow
13 response. The event presents a unique opportunity for a detailed study as it occurred
14 during a period of special observations made at the center of a rain gauge network
15 recently installed in and near the Great Smoky Mountain National Park in western North
16 Carolina.

17

18 The evolution of rainfall intensity during this ordinary event occurred under conditions
19 that typically push the limits of applicability in making QPEs based on Z-R algorithms.
20 Several convective cells that developed over eastern Tennessee and propagated into the
21 study domain produced the rainfall observed by a rain gauge network in the southern
22 Appalachian Mountain region. This case study is particularly challenging from a QPE
23 perspective because the event cuts across several different categories typically used in
24 defining appropriate Z-R relationships. Specifically, this event evolves as an initially
25 convective rainfall event associated with thunderstorms over Tennessee that propagate
26 over an orographic barrier, dumping precipitation into a high elevation rain gauge
27 network, and change their intensity to stratiform rainfall rates as they reach their end.
28 Hence, this event has potential applications for the following general Z-R relationship
29 categories; stratiform rain, thunderstorm, orographic precipitation, and showers, all
30 defined by Ulbrich (1983).

1
2
3
4
5
6
7
8
9
10
11
12
13
14
15
16
17
18
19
20
21
22
23
24
25
26
27
28
29
30

1.1 The Great Smoky Mountain Rain Gauge Network

A rain gauge network has been installed in Haywood County of western North Carolina (Figure 1) in a remote region bordered by the Blue Ridge Mountains to the east and the Great Smoky Mountains to the west. Installation of the Great Smoky Mountain Rain Gauge Network (GSMRGN, Table 1) started in the summer 2007 and currently {as of 12 June 2009} consists of 32 tipping bucket rain gauges in Haywood County, representing the south-central portion of the Pigeon River Basin (inset of Figure 1). Twelve tipping bucket gauges were recently installed (locations not shown) directly in the Great Smoky Mountain National Park (GSMNP) in the summer 2009 which completes the sampling of the highest elevation locations within the Pigeon River Watershed. Seven of these gauges are positioned along a ridgeline collocated with the well-traveled Appalachian Trail that follows the eastern Tennessee and western North Carolina border.

A special intensive observation campaign took place from 22 – 30 July 2008 within Haywood County at the National Park Service research facility located near Purchase Knob. The facility has a surface elevation of almost 1500 meters and is located along the Cataloochee Divide (red circle on inset of Figure 1), bordering the GSMNP. Special instrumentation installed for the campaign consisted of a vertically-pointing micro-rain radar (MRR), a disdrometer, a tethersonde with sensors installed for measuring boundary layer vertical profiles of temperature, moisture, pressure and winds, a high-speed camera for photographing the shapes of falling raindrops, and a GPS-based mobile rawinsonde system. Weather balloon launches occurred every three hours starting at 1500 UTC 25 July 2008 until the end of the intensive observation period. The results presented in this study focus on a precipitation event that impacted the mountains of Haywood County starting in the afternoon of July 28 and ending in the early morning hours of July 29.

The instantaneous stream flow at three United States Geological Survey (USGS) stream gauges (labeled ‘00’, ‘07’, and ‘15’ on Figure 1) located toward the downstream portion of the Pigeon River Basin are shown in Figure 2 covering a four day period. Furthest

1 upstream and away from the main stem of the Pigeon River, the USGS stream gauge on
2 Cataloochee Creek ('00' on Figure 1) responds to the precipitation generated by the
3 ordinary thunderstorms that occurred on July 28 and 29 when its discharge rate nearly
4 doubles from a "normal" flow rate of 24 to 41 cfs at 0700 Eastern Daylight Time (EDT,
5 1100 UTC) on July 29 (Figure 2a). The cumulative impact of sub-basin drainage into the
6 Pigeon River can be observed in the stream flow at a gauge located near Waterville, NC
7 ('07' on Figure 1). The discharge rate increases *dramatically* from a normal flow rate of
8 ~160 cfs to a peak near 1100 cfs at 1145 EDT (1545 UTC) 29 July in response to the
9 passage of the thunderstorms (Figure 2b). The over five-fold increase in stream flow rate
10 at gauge '07' continues for a period of nearly four hours. Further downstream along the
11 Pigeon River, stream flow at Newport, TN ('15' on Figure 1) also increases substantially
12 in response to the run-off of precipitation generated by the passage of the ordinary
13 thunderstorms. The normal flow rate of ~185 cfs at Newport, TN increases to a peak of
14 just over 1000 cfs at 1900 EDT (2300 UTC) 29 July and endures for almost two hours
15 before gradually subsiding (Figure 2c).

16

17 This case study illustrates in detail the impact that a sequence of rather ordinary
18 thunderstorms can have on the hydrological response at various spatial scales for
19 mountainous regions and highlights the importance in making accurate orographic QPEs.
20 The process from initial rainfall to flash flooding in the southern Appalachian Mountains
21 is not well understood owing to the lack of *in situ* high elevation surface-based direct
22 point observations and imperfect remote measurements typical of a mountainous region.
23 This study is the first in a series associated with observations collected as part of a pro-
24 active approach to natural hazard management, to improve our understanding of flash
25 flooding in the southern Appalachians so that warning accuracy and lead times can be
26 increased for these events that are not uncommon, are poorly understood, and often go
27 undetected. The remainder of the manuscript is organized as follows. First, a summary of
28 the synoptic-scale weather pre-cursor conditions of the 28, 29 July 2008 is described in
29 Section 2. Second, a description of the mesoscale weather conditions for eastern
30 Tennessee and western North Carolina during the 28, 29 July 2008 is provided in Section

1 3. An analysis of the weather event on the scale of an individual watershed is given in
2 Section 4 and a summary of the findings and their relevance to making QPEs in
3 mountainous regions of the mid-latitudes is described in Section 5.

4 5 **2. Synoptic conditions**

6 The synoptic-scale conditions leading to the 28 July 2008 precipitation event in western
7 North Carolina consist of a ridge of high pressure dominating the central and western
8 United States (Figure 3) and a trough located over the eastern United States. A relative
9 maximum in absolute vorticity is evident over eastern Iowa at 0000 UTC 28 July (Figure
10 3a) and proceeds to dip southeastward as it exits the ridge and enters the trough,
11 weakening as it moves toward Kentucky by 1800 UTC 28 July (Figure 3b). The absolute
12 vorticity maximum is associated with a mesoscale convective system (MCS) that caused
13 wind and hail damage and produced five tornado reports in Iowa, Illinois, and Missouri
14 as documented by the Storm Prediction Center (SPC) on 27 July (SPC 2008). The 0120
15 UTC 28 July SPC mesoscale discussion indicates that some of the storms located along
16 the convective line had supercell characteristics, dropping hail as large as four inches in
17 diameter, and producing wind gusts near 70 miles per hour (SPC 2008).

18
19 The cloud mass associated with the MCS located over eastern Iowa at 0000 UTC 28 July
20 is evident in the Geostationary Operational Environmental Satellite (GOES) 12 IR image
21 (Figure 4a). Also evident at this time is the cloud mass located along the U.S. East Coast
22 associated with the trough at the 850 hPa level. By 1800 UTC 28 July the easternmost
23 absolute vorticity maximum fragment (Figure 3b) is now located in close proximity to a
24 newly forming convective cell evident over eastern Kentucky (Figure 4b).

25 26 **3. Mesoscale discussion**

27 Evolution of the mesoscale weather elements that contributed to the rainfall observed in
28 western North Carolina on 28 July was examined carefully using time loops of NEXt
29 Generation Weather RADar (NEXRAD) Level II data archived by the National Climatic
30 Data Center (NCDC) for the sites located in Jackson, Kentucky (KJKL), Knoxville,

1 Tennessee (KMRX), and Greer, South Carolina (KGSP). Examination of the NEXRAD
2 Level II data focused on evolution of the mesoscale weather elements as indicated using
3 the base reflectivity imagery.

4
5 Cluster 1 (C1, Figure 5a) represents convection directly related to the remnants of the
6 MCS from the previous day, reaching its peak at 1445 UTC 28 July. Outflow from C1 is
7 seen in the NEXRAD imagery to contribute to the development of Cluster 2 (C2) which
8 is intensifying at the time of the image shown in Figure 5a. C2 is evident as the green
9 spot of growing convection located over eastern Kentucky in the IR imagery of Figure
10 4b. Cluster 3 (C3) is barely noticeable at the time of Figure 5a (1700 UTC 28 July),
11 grows and splits into a northward (C3n) and southward (C3s) propagating cluster of
12 convection. The C2 and C3n clusters merge at 1854 UTC 28 July and are responsible for
13 a severe thunderstorm observed in eastern Kentucky at 1900 UTC 28 July. The C3s
14 convection cluster passes over gauge #111 (red square on inset of Figure 1) and is
15 responsible for the first precipitation event observed by the GSMRGN on 28 July at 2055
16 UTC. The genesis of C2 and C3 is aided by lift forced from cyclonic vorticity advection
17 at the 500 hPa level occurring downstream of the remnant MCS absolute vorticity
18 maximum (Figure 3b).

19
20 The merger between C2 and C3n (C2-C3n, Figure 5b) has almost crossed into North
21 Carolina by 2124 UTC 28 July and new convection has developed in central Kentucky
22 (C4a) and in central (C4b) and eastern (C5) Tennessee. The C2-C3n merger stalls
23 somewhat after crossing into North Carolina and is responsible for two rainfall events
24 observed at gauge #111 around 2300 UTC 28 July. The two C4 clusters encircled by the
25 oval in Figure 5b merge by 2220 UTC 28 July and merges with C5 by 2250 UTC 28 July
26 and slowly begin to cross into North Carolina at 23:03 UTC 28 July. The slow-moving
27 C4-C5 merger is responsible for a majority of the rainfall observed in Haywood County
28 at most locations in the GSMRGN on 28 July, with peak rainfall occurring at 0200 UTC
29 29 July and the rear flank of the cluster passing over the southernmost gauges by 0400
30 UTC 29 July.

1

2 At 2100 UTC 28 July (Figure 6a), C3s is overhead gauge #111 and the C2-C3n merger
3 has moved into eastern Tennessee and the cloud tops have warmed on average from -55
4 to -45°C during the period. The corresponding NEXRAD image from KMRX (Figure 7a)
5 shows the hydrometeors associated with the C2-C3n merger to the north and those
6 associated with the C3s cluster overhead gauge #111. No other gauges of the GSMRGN
7 are reporting rainfall at this time.

8

9 The cloud tops associated with the C2-C3n merger continue to warm as the cluster has
10 moved into western Virginia and North Carolina (Figure 6b) by 0000 UTC 29 July.
11 Convection associated with the C4-C5 merger at this time is quite vigorous as indicated
12 by the cold cloud tops (-57°C) located over eastern Tennessee. The C4-C5 convection is
13 completely missed by the KMRX NEXRAD imagery (Figure 7b) since it is practically
14 located overhead the radar station (far upper left corner of the figure). The precipitation
15 observed at gauge #111 at 2349 UTC 28 July is falling from the stalled remnants of the
16 C2-C3n merger.

17

18 Convection associated with the C4-C5 merger falls apart as it crosses the mountains of
19 western North Carolina, reflected in warm cloud top temperatures (-47°C) at 0200 UTC
20 29 July (Figure 6c). By this time the precipitation has spread over the entire GSMRGN
21 and is stratiform in nature (Figure 7c), evident in the relatively low base reflectivity
22 values observed by the KGSP NEXRAD station. The slow-moving cluster impacts the
23 southernmost gauges of the GSMRGN two hours later (0400 UTC 29 July) as the cloud
24 tops warm and continue to become disorganized (Figure 6d). By this time, the
25 northernmost gauges of the GSMRGN (Figure 7d) have stopped observing precipitation
26 associated with the group of convective clusters spawned on 28 July 2008.

27

28 A series of rawinsondes were launched from Purchase Knob (red circle on inset of Figure
29 1) as a part of the July 2008 intensive observation period to assess the evolving stability
30 and moisture fields. In addition, a tetheredsonde was deployed giving vertical

1 meteorological profiles within 100 meters of the surface. Rawinsonde (Figure 8a) and
2 tethersonde (not shown) data valid at 1500 UTC 28 July indicate a rather dry atmosphere
3 with a relative humidity at 100m above ground level (AGL) around 55%. At 2100 UTC
4 28 July, observer notes at Purchase Knob indicate convective storms to the north, but no
5 precipitation, while the sounding data (Figure 8b) indicates a cloud deck at or near the
6 500 hPa level and an increase of moisture within the atmospheric boundary layer. The
7 2100 UTC temperature profile at Purchase Knob shows a well-mixed boundary layer
8 from the ground up to the 750 hPa level and a good potential for convection if low-level
9 processes can moisten the boundary layer sufficiently and achieve lift of surface-based
10 parcels. The temperature profile at Purchase Knob at 0000 UTC 29 July (Figure 8c)
11 indicates a modest stabilization of the upper boundary layer and observer notes indicate
12 overcast conditions, no precipitation, and light winds at the surface. Unfortunately, the
13 moisture sensor malfunctioned just after launch and no direct moisture profile
14 information for Purchase Knob can be obtained at 0000 UTC 29 July. By 0300 UTC 29
15 July (Figure 8d) the atmosphere at Purchase Knob is nearly saturated through a deep
16 layer (throughout the troposphere) and the entire boundary layer has stabilized. Observer
17 notes valid at 0300 UTC indicate rain falling at Purchase Knob, likely associated with the
18 dying remnants of the C4-C5 cluster.

19

20 **4. Pigeon River Watershed discussion**

21 Accumulated precipitation as measured by the GSMRGN (Figure 9) indicates a
22 maximum accumulation at gauge #111 of just over 21 millimeters (mm) to amounts
23 below 5 mm toward the southern region of the gauge network (Figure 10). Precipitation
24 associated with three distinct events at gauge #111 is noted in Figure 9 and corresponds
25 to the times of the images shown in Figures 6a-c and Figures 7a-c. Passage of the C3s
26 and C2-C3n events occurred toward the northern edge of the network so that their
27 passage is only noted by gauge #111. In contrast, every gauge registered precipitation
28 associated with the C4-C5 event since it moved toward the southeast (Figures 6c, 6d, 7c,
29 and 7d) as it crossed the mountains from Tennessee. The operational rain gauges
30 indicated by green circles in Figure 10 are operated by the Tennessee Valley Authority

1 (TVA) and the USGS and are found in the valleys of Haywood County (elevation [z]
2 range of 1500-2000 feet). A large rainfall contrast can be seen in the southwestern
3 portion of the GSMRGN in Figure 10 where an operational gauge (WAVN7) observed an
4 accumulation of 5.6 mm compared to 18.0 mm for GSMRGN gauge #106 located near
5 Pinnacle Ridge within a distance of less than 3.2 km. These results are consistent with the
6 general notion that gauges in valleys underestimate accumulated precipitation (Barros et
7 al. 2000).

8

9 The remaining discussion focuses on observations made near Purchase Knob for the 28,
10 29 July 2008 event, corresponding to the location of gauge #100 (red circle on inset of
11 Figure 1). The MRR in place during the event compared with observations made by
12 gauge #100 shows a strong correlation between the rainfall rates estimated by the tipping
13 bucket gauge and the MRR during the period of heaviest rainfall (0132 – 0242 UTC 29
14 Jul 2008). The agreement between the two sources diminishes as the C4-C5 event decays
15 and the precipitation falls primarily with rates below 5.0 mm h^{-1} (0242 – 0331 UTC 29
16 Jul 2008). This lack of agreement is consistent with the challenge of inferring rainfall
17 from radar reflectivity for small rainfall rates (Prat and Barros 2009). No significant
18 rainfall is observed to exist by either the rain gauge or the MRR at Purchase Knob after
19 0530 UTC 29 Jul 2008.

20

21 A comparison of gauge #100 rainfall with GOES 12 brightness temperature (Tb)
22 observations at channels 3, 4, and 6 for the period 0100 through 0548 UTC 29 Jul 2008
23 reveals three interesting features for the GOES 12 pixels located nearest Purchase Knob;
24 the overall warming of the Tbs during the 0100 – 0548 UTC period, the increasing spread
25 in the Tbs between the three channels over the five hour period, and a “sudden” warming
26 in the Tbs at 0212 UTC. The overall warming at the GOES 12 IR channels is indicative
27 of the warming cloud top temperatures associated with weakening convection as it passes
28 overhead of Purchase Knob, typical for convection as the event evolves further from
29 sunset (about 0030 UTC). The increasing spread in the Tbs between the three IR channels
30 is indicative of the decreasing opacity of the cloud, also associated with a thinning of the

1 convective clouds as they decay over the five-hour period. The “sudden” warming is
2 observed to occur as gauge #100 is experiencing its heaviest precipitation during the
3 study period, centered at 0212 UTC. It appears that the cell overhead Purchase Knob has
4 had a significant decrease in its updraft, allowing a significant number of the previously
5 suspended hydrometeors to fall out of the cloud. Unfortunately, a secondary peak in
6 rainfall observed by gauge #100 at 0307 UTC occurs at a time that there is a gap in the
7 GOES 12 IR Tb data archive. A comparison of the Tb time series to the rainfall observed
8 at gauge #100 shows a rather poor correlation, hence, QPEs based on GOES 12 IR Tbs
9 alone for channels 3, 4, and 6 shows little utility.

10
11 A comparison of gauge #100 rainfall with NEXRAD base reflectivity (dBz) from the
12 KGSP and KMRX stations (locations plotted in Figure 1) is displayed in Figure 11 for
13 the period 0100 through 0548 UTC 29 Jul 2008. NEXRAD reflectivities were examined
14 at the lowest five elevation angles for both locations and those elevation angles of 1.37°
15 and 2.44° provided the greatest dynamic variance over the 28, 29 Jul 2008 precipitation
16 for KGSP and KMRX, respectively. In general, the reflectivities from both locations
17 correlate well with the rainfall rate observed at gauge #100, the exception being for the
18 lighter amounts associated with the decaying phase of the C4-C5 event. The 64 (72) 1.37°
19 (2.44°) elevation angle reflectivity scans for KGSP (KMRX) over the period have a mean
20 of 21.3 (23.0) dBz and a standard deviation of 11.4 (12.1) dBz. It is important to bear in
21 mind that the KGSP lowest elevation scan is located about 2 km above sea level at
22 Purchase Knob while it is at an altitude of 1.5 km above sea level for KMRX. Hence, the
23 lowest elevation angle scan from KGSP (KMRX) is 500 (100) meters above ground level
24 at Purchase Knob whose surface elevation is almost 1495 meters. The 1.37° (2.44°)
25 elevation angle reflectivity scans for KGSP (KMRX) are at a mean elevation of 3610
26 (3700) meters above sea level, so the reflectivities at these elevation angles are located
27 about 1100 (1200) meters above ground level. For reference, the MRR-derived fall
28 velocities and reflectivity for the 28, 29 Jul 2008 event (Figure 12) indicate that the
29 melting level is well above 1.1-1.2 km above ground level at Purchase Knob. The 0000

1 UTC 29 Jul 2008 sounding observation at Purchase Knob (Figure 8c) indicates the
2 freezing level to be at an elevation of 4.485 km, almost 3000 meters above ground level.

3
4 Reflectivities observed at the KGSP (elevation angle = 1.37°) and KMRX (elevation
5 angle = 2.44°) NEXRAD stations for the 28, 29 July 2008 are used to estimate rainfall
6 rate (mm h^{-1}) using seventeen Z-R algorithms (Table 3) included in Figures 3 and 11 of
7 Prat and Barros (2009) and are plotted at the appropriate times in Figure 13. These
8 algorithms (total number of algorithms) represent the “Stratiform” (4), “Thunderstorm”
9 (4), “Orographic” (3), and “Showers” (4) categories of Ulbrich (1983) in addition to two
10 TRMM algorithms strictly designed for tropical applications. The observed rainrates
11 plotted in Figure 13 (solid lines) are the mean of the gauge #100 observations occurring
12 within two minutes of each NEXRAD sweep. There are, at most, three gauge “tips”
13 contributing to the mean rainrate observation calculations during this particular event.

14
15 Most Z-R algorithms represent a significant overestimation of the observed rainrate as
16 seen by the cloud of points in Figure 13 residing above the observed rainrate line. The
17 overestimation tendency appears to be worse for the KMRX reflectivity observations
18 (Figure 13b) than for those at KGSP. The reason for the discrepancy in performance
19 between the two NEXRAD stations is hypothesized to be that the beams are looking at
20 slightly different levels and angles of the precipitating cloud. It is unknown if the
21 discrepancy represents a significant difference. If we focus on the Z-R algorithm points
22 found in close proximity to the observed rainfall trace in Figure 13, we find that the best
23 Z-R QPE performance at the time of each NEXRAD sweep varies between several
24 different algorithms over the focus period, consistent with the motivation for the Prat and
25 Barros (2009) paper that no single Z-R algorithm gives an obvious best performance over
26 the duration of a precipitation event.

27
28 If we filter the seventeen Z-R algorithms down to those having the most consistent
29 performance and adjust for slight time discrepancies between the NEXRAD and gauge
30 #100, we find estimates giving reasonable approximations as plotted in Figure 14. The

1 “best” Z-R algorithm ($Z = 520 \times R^{1.81}$; Foote 1966, indicated by the trace having the “x”
2 characters) comes from the “Showers” category and represents a correlation of 0.68
3 (0.64) for the 24 (23) comparison data pairs of the KGSP (KMRX) reflectivity
4 observations over Purchase Knob (Table 2). Another Z-R algorithm of comparable
5 performance for this case using rainfall observations at Purchase Knob comes from the
6 “Thunderstorms” category ($Z = 450 \times R^{1.48}$; Fujiwara 1965, indicated by the trace having
7 the square characters). Both algorithms generally suffer from an underestimation of the
8 rainrate, particularly during periods when the observed rainrate is in the 2 – 6 mm h⁻¹
9 range. The negative biases would lead one to conclude that less precipitation had
10 accumulated at Purchase Knob using QPEs based on NEXRAD reflectivities than what
11 had actually occurred. The variation in performance of both Z-R algorithms over the
12 0100 – 0324 UTC 29 July 2008 period again confirms the contention of Prat and Barros
13 (2009) that changing microphysical properties of precipitation-producing clouds makes
14 the application of a single Z-R algorithm for QPEs of a storm misguided, at best.

15

16 **5. Summary**

17 The remnants of a MCS from Iowa (C1) and its associated absolute vorticity pre-
18 conditioned the environment in eastern Kentucky and Tennessee for convection that
19 developed just before mid-day (1700 UTC) on 28 July 2008 (C2). This convection
20 merged with a northward-propagating cluster of convection (C3n) at 1854 UTC 28 July
21 that resulted in a severe thunderstorm being observed in eastern Kentucky at 1900 UTC
22 28 July. A southward-propagating cluster of convection (C3s) initiated the sequence of
23 precipitation observed by the GSMRGN as it passed over gauge #111 at 2055 UTC. The
24 C2-C3n merger crossed into western North Carolina and passed over gauge #111 around
25 2300 UTC. In the meantime, new convection in Kentucky (C4a) and central Tennessee
26 (C4b) merged at 2200 UTC and the newly organized system merged with other new
27 convection that had initiated in eastern Tennessee (C5) at 2250 UTC. The C4-C5 merger
28 crossed into western North Carolina, propagating toward the southeast and was
29 responsible for most of the precipitation accumulation observed by the GSMRGN,
30 peaking at about 0200 UTC 29 July 2008. GOES 12 IR observations indicate that the

1 C3s, C2-C3n, and C4-C5 convection mergers became disorganized as they crossed the
2 mountains bordering western North Carolina, evident by the warming cloud top
3 temperatures as orography was being traversed.

4
5 Rawinsondes launched before and during passage of the 28, 29 July convection near
6 Purchase Knob indicated an evolution of the boundary layer stabilization from neutral at
7 2100 UTC 28 July to an increasing stability at the boundary layer top at 0000 UTC 29
8 July and throughout the boundary layer by 0300 UTC 29 July. Observations of near
9 surface relative humidity available from the rawinsonde launches and a tethersonde
10 indicated a dry atmosphere (~55%) at mid-day on 28 July. Much of the initial
11 precipitation hydrometeors falling overhead of Purchase Knob likely evaporated and
12 moistened the lower atmosphere before the first observation of precipitation at the ground
13 was detected at gauge #100 at 0124 UTC 29 July.

14
15 The observed total accumulated precipitation for the 28, 29 July 2008 event for the
16 GSMRGN ranged from just below 5 mm at gauge #1 to just above 21 mm (0.83 inches)
17 at gauge #111 over a period of nine hours (2100 UTC 28 July through 0600 UTC 29 July
18 2008). The highest accumulation occurred at gauge #111 during this event because it was
19 the only location in the GSMRGN to be impacted by the precipitation of three distinct
20 convective cells or mergers (C3s, C2-C3n, and C4-C5). Rain gauges located in close
21 proximity but at significantly different elevations showed higher accumulation amounts
22 for the higher elevation stations, consistent with observations described in Barros et al.
23 (2000). The net basin-wide impact of the passage of ordinary thunderstorms on 28, 29
24 July 2008 yielded a five-fold increase in the stream discharge rates as noted at two
25 gauges sites located along the Pigeon River on the downstream side of the Pigeon River
26 Watershed. The ordinary thunderstorms that developed on July 28 are common for this
27 region during the warm season, forming in environments that usually prompt no special
28 weather watches (e.g. severe thunderstorm or tornado) or mesoscale discussions by the
29 SPC.

30

1 The observed precipitation intensity at gauges #100 and 111 reached maximum values
2 over the nine-hour period of 11.4 and 52.0 mm h⁻¹, respectively, on the moderate-to-low
3 end of the rainrate spectrum. Examination of remote measurements often used in QPE
4 algorithms made during the 28, 29 July event provided several revealing insights.
5 Observations of reflectivity over Purchase Knob at the 1.37° and 2.24° elevation angle
6 scans of the KGSP and KMRX NEXRAD stations, respectively, during this event gave
7 the optimal dynamic range as they scanned into the clouds at an elevation of about 1.1
8 km above ground level. Using these reflectivity observations as input for seventeen Z-R
9 algorithms revealed that one of the “Showers” and one of the “Thunderstorms”
10 algorithms defined in Prat and Barros (2009) provided a fair representation of the rainfall
11 rates observed near Purchase Knob. However, as rainfall intensity dropped below 6 mm
12 h⁻¹, the two Z-R algorithms consistently underestimated the observed rainfall intensity
13 near Purchase Knob. The poor overall performance of the two Z-R algorithms for the
14 case study is hypothesized to be a result of the non-steady state conditions of the cloud
15 microphysical properties. The changing cloud top properties for the 28, 29 July 2008
16 event and, by implication, the changing cloud microphysical properties are confirmed by
17 the GOES 12 IR observations that indicate warming (lowering) of cloud tops as the
18 convective systems move east. The transient evolution of the cloud droplet size
19 distribution, a result of non-steady state conditions between the processes of
20 condensation, evaporation, coalescence, breakup, and accretion, is the motivation for a
21 re-examination of radar rainfall estimation as proposed in Prat and Barros (2009).

22

23 The data base being developed as part of the GSMRGN will be used to train operational
24 forecasters and test various geophysical models to aid in improving flash flood warnings
25 in mountainous regions. Examination of the 28, 29 July 2008 case study represents an
26 initial step into measuring and understanding orographic precipitation regimes and
27 hydrology in the southern Appalachian Mountains. The case raises several questions that
28 will serve to guide the ongoing study in this unique region of the globe. One pursuit will
29 be the investigation of the applicability of the results to case studies having distinctly
30 different rainrate intensities (heavy rainfall) and cloud structure (non-convective,

1 stratiform). Another pursuit will be to use high resolution model simulations to
2 investigate the impact of model physics (e.g. microphysics) closure assumptions on
3 Quantitative Precipitation Forecasts and to better understand precipitation accumulation
4 differences for gauges having similar elevations within close proximity. Figure 10 shows
5 a surprising amount of variance in the event observed precipitation accumulation [OPA]
6 between the five GSMRGN gauges clustered along the Cataloochee Divide ridgeline
7 stretching from northeast to southwest starting at gauge #100 (OPA = 9.4 mm) to gauge
8 #101 (OPA = 11.4 mm) to gauge #102 (OPA = 17.7 mm) to gauge #103 (OPA = 19.2
9 mm) to gauge #110 (OPA = 16.4 mm). Of particular interest will be to examine model
10 simulations for evidence of mesoscale flow patterns that may explain the localized
11 enhancements of precipitation evident at gauge #103 and near Pinnacle Ridge (gauge
12 #106). A third pursuit will represent a blend of high resolution modeling efforts with
13 available observations later in the day on 29 July 2008 to investigate the potential pre-
14 conditioning role that the event studied in this manuscript played in initiating local
15 convection that impacted the southeastern portion of the GSMRGN on 29, 30 July 2008.

16

17 **Acknowledgements**

18 This research was supported in part by NASA grant NNX07AK40G at Duke University.
19 Additional support for rawinsonde launches was provided by internal funds from the Pratt
20 School of Engineering at Duke University. The authors are grateful to Paul Super and
21 Susan Sachs of the National Park Service, and to Do Hyuk Kang, Prabahkar Shrestha,
22 We Li, Kun Tao, Julien Brun, and Rojina Manandhar for their support during the July
23 2008 field campaign. The authors also wish to thank Dr. Dongsoo Kim of NCDC for
24 providing operational rain gauge data as part of the HADS project. The MRR unit used
25 during the IOP in 2008 was on loan from the RENaissance Computing Institute (RENCI)
26 and the authors are grateful to Jessica Proud, Erik Scott, Mats Rynge, and Ken Galluppi
27 for assisting in its operation. Finally, the authors wish to thank Dr. Phil Durkee and Mr.
28 Richard Lind of the Naval Postgraduate School for loaning the MRS sounding unit used
29 during the IOP in 2008 and for offering technical expertise in its operation.

30

31

1 **References**

- 2 Barros, A.P., and Lang, T.J.: Monitoring the monsoon in the Himalayas: Observations in
3 central Nepal, June 2001. *Mon. Wea. Rev.*, **131**, 1408-1427, 2003.
- 4 ———, A.P., Joshi, M., Putkonen, J., and Burbank, D.W.: A study of the 1999 monsoon
5 rainfall in a mountainous region in central Nepal using TRMM products and rain gauge
6 observations. *Geophys. Res. Lett.*, **27**, 3683-3686, 2000.
- 7 ———, A.P., Kim, G., Williams, E., and Nesbitt, S.W.: Probing orographic controls in
8 the Himalayas during the monsoon using satellite imagery. *Nat. Hazards Earth Syst.*, **4**,
9 1-23, 2004.
- 10 Battan, L.J.: *Radar Observation of the Atmosphere*. University of Chicago Press, 324 pp.,
11 1973.
- 12 Bhushan, S. and Barros, A.P.: A numerical study to investigate the relationship between
13 moisture convergence patterns and orography in central Mexico. *J. Hydrometeor.*, **8**,
14 1264-1284, 2007.
- 15 Brock, F.V. and Richardson, S.J.: *Meteorological Measurement Systems*. Oxford
16 University Press, 290 pp., 2001.
- 17 Cecil, D.J., Goodman, S.J., Boccippio, D.J., Zipser, E.J., and Nesbitt, S.W.: Three years
18 of TRMM precipitation features. Part I: Radar, radiometric, and lightning distributions.
19 *Mon. Wea. Rev.*, **133**, 543-566, 2005.
- 20 Douglas, E.M. and Barros, A.P.: Probable maximum precipitation estimation using
21 multifractals: Application in the eastern United States, *J. Hydrometeor.*, **4**, 1012–1024,
22 2003.
- 23 Foote, G.B.: A Z-R relation for mountain thunderstorms. *J. Appl. Meteor.*, **2**, 229-231,
24 1966.
- 25 Fujiwara, M.: Raindrop-size distribution from individual storms. *J. Atmos. Sci.*, **22**, 585-
26 591, 1965.
- 27 National Weather Service (NWS):
28 <http://www.erh.noaa.gov/gsp/localdat/cases/Frances2004/frances.htm> , 2004a.
29 National Weather Service (NWS):
30 <http://www.erh.noaa.gov/gsp/localdat/cases/Ivan2004/ivan.htm> , 2004b.

1 Nesbitt, S.W., Cifelli, R., Rutledge, S.A., Boccippio, D.J., Cecil, D.J., and Zipser, E.J.:
2 The horizontal structure of precipitating systems in the Tropics according to TRMM.
3 *Preprint volume, 2nd TRMM International Science Conference, Nara, Japan, 2004.*
4 Prat, O.P. and Barros, A.P.: Exploring the transient behavior of Z-R relationships-
5 Implications for radar rainfall estimates. *J. of Applied Meteor. and Clim.* In press, 2009.
6 Raghavan, S.: *Radar Meteorology*. Kluwer Academic Publishers, 549 pp., 2003.
7 Storm Prediction Center (SPC):
8 <http://www.spc.noaa.gov/exper/archive/events/080727/index.html> , 2008.
9 Ulbrich, C.W.: Natural variations in the analytical form of the raindrop size distribution.
10 *J. Climate Appl. Meteor.*, **22**, 1764-1775, 1983.
11
12
13
14
15
16
17
18
19
20
21
22
23
24
25
26
27
28

1 Table 1: The Great Smoky Mountain Rain Gauge Network is currently (valid as of 12
 2 June 2009) comprised of 32 tipping bucket rain gauges. Highlighted gauges are
 3 frequently referenced locations in the manuscript.

Gauge #	Location	Latitude	Longitude	Altitude
RG001	Deep Gap	35°23.8' N	82°54.7' W	3794 ft.
RG002	Lickstone Bald	35°25.5' N	82°58.2' W	5680 ft.
RG003	High Top	35°23.0' N	82°54.9' W	5280 ft.
RG004	Lickstone Ridge S	35°22.0' N	82°59.4' W	6305 ft.
RG005	Deep Gap	35°24.5' N	82°57.8' W	4986 ft.
RG008	Double Spring Gap	35°22.9' N	82°58.4' W	5700 ft.
RG010	Beaty Spring Gap	35°27.3' N	82°56.8' W	4849 ft.
RG100	Purchase Knob	35°35.1' N	83°04.3' W	4905 ft.
RG101	The Swag	35°34.5' N	83°05.2' W	4986 ft.
RG102	Hemphill Bald	35°33.8' N	83°06.2' W	5365 ft.
RG103	JR Property	35°33.2' N	83°07.0' W	5539 ft.
RG104	Cat. Ski Area	35°33.2' N	83°05.2' W	5208 ft.
RG105	KH Property	35°38.0' N	83°02.4' W	4412 ft.
RG106	Pinnacle Ridge	35°25.9' N	83°01.7' W	3969 ft.
RG107	Lookout Point	35°34.0' N	82°54.4' W	4459 ft.
RG108	Utah Mountain	35°33.2' N	82°59.3' W	4188 ft.
RG109	Eaglesnest Ridge	35°29.7' N	83°02.4' W	4922 ft.
RG110	JH Property	35°32.8' N	83°08.8' W	5128 ft.
RG111	Hurricane Ridge	35°43.7' N	82°56.8' W	4573 ft.
RG112	Ore Knob	35°45.0' N	82°57.8' W	3884 ft.
RG300	Camel Hump Knob	35°43.5' N	83°13.0' W	5110 ft.
RG301	Mt Guyot	35°42.3' N	83°15.3' W	6570 ft.
RG302	Snake Den Ridge	35°43.2' N	83°14.8' W	6104 ft.
RG303	Mt Cammerer	35°45.7' N	83°09.7' W	4887 ft.
RG304	Big Cataloochee	35°40.2' N	83°10.9' W	5971 ft.
RG305	Mt Sterling 1	35°41.4' N	83°07.9' W	5349 ft.
RG306	Sunup Knob	35°44.7' N	83°10.2' W	5039 ft.
RG307	Balsam Mountain	35°39.0' N	83°11.9' W	5327 ft.
RG308	Cosby Knob	35°43.8' N	83°10.9' W	4826 ft.
RG309	Mt Sterling 2	35°40.9' N	83°09.0' W	5262 ft.
RG310	Mt Sterling 3	35°42.1' N	83°07.3' W	5761 ft.
RG311	Big Creek	35°45.9' N	83°08.4' W	3398 ft.

4
 5
 6
 7
 8

1 Table 2: Statistics for rain rate (mm h^{-1}) as observed by the Great Smoky Mountain Rain
 2 Gauge Network gauge #100 (G#100) located at Purchase Knob in the Pigeon River
 3 Watershed and estimated rain rate (mm h^{-1}) based on Z-R relationships for “Showers”
 4 ($A=520$, $b=1.81$) and for “Thunderstorms” ($A=450$, $b=1.48$, “T-storms”) as defined in
 5 Prat and Barros (2009) for reflectivity (dBz) observed from the KGSP (elevation
 6 angle= 1.37°) and KMRX (elevation angle= 2.44°) NEXRAD sites over the period 0100
 7 UTC through 0324 UTC 29 July 2008.

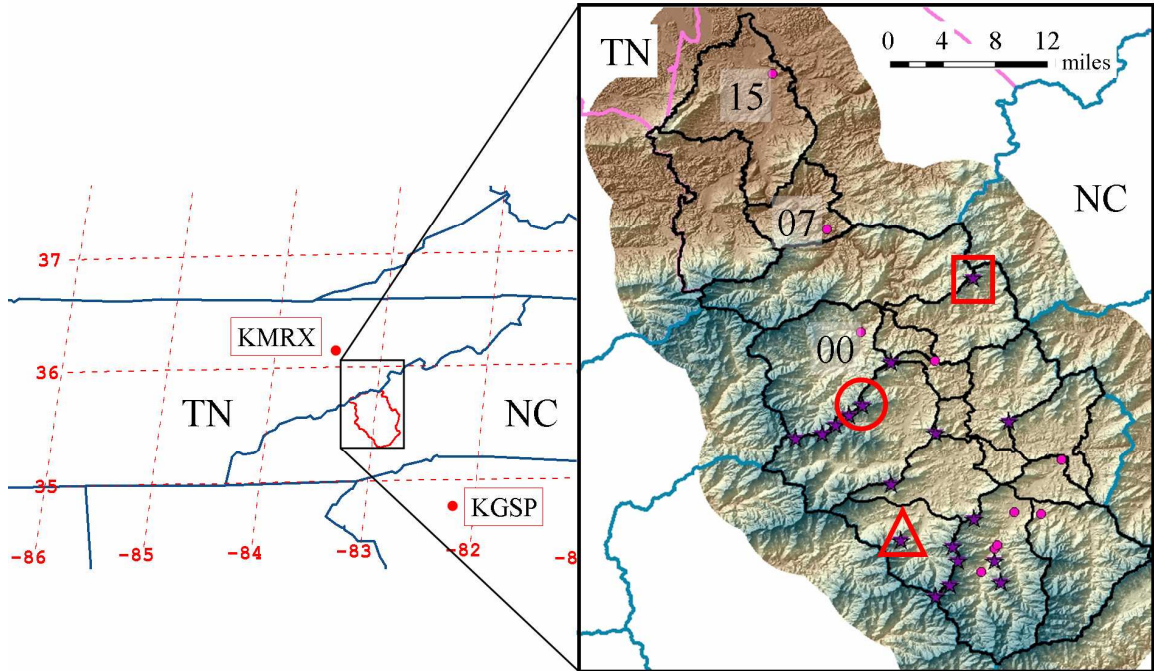
Algorithm	Station	G#100 mean (mm h^{-1})	G#100 σ (mm h^{-1})	QPE mean (mm h^{-1})	QPE σ (mm h^{-1})	RMSE (mm h^{-1})	Bias (mm h^{-1})	R^2	N
Showers	KGSP	4.64	2.56	2.48	2.05	2.88	-2.16	0.68	24
Showers	KMRX	4.74	2.60	3.28	1.99	2.49	-1.46	0.64	23
T-storms	KGSP	4.64	2.56	3.63	3.71	2.97	-1.01	0.66	24
T-storms	KMRX	4.74	2.60	4.93	3.66	2.83	+0.19	0.64	23

8
 9
 10
 11
 12
 13
 14
 15
 16
 17
 18
 19
 20
 21
 22
 23
 24
 25
 26
 27
 28
 29
 30
 31
 32
 33
 34

1 Table 3: [A, b] coefficients of the seventeen Z-R relationships tested using the KMRX
2 (elevation angle=2.44°) and KGSP (elevation angle=1.37°) NEXRAD reflectivity
3 observations at Purchase Knob over the period 0100 UTC through 0324 UTC 29 July
4 2008.

Category	A	b
Stratiform	200.	1.60
Stratiform	205.	1.48
Stratiform	255.	1.41
Stratiform	313.	1.25
Thunderstorm	486.	1.37
Thunderstorm	290.	1.41
Thunderstorm	219.	1.41
Thunderstorm	450.	1.48
Orographic	31.	1.71
Orographic	109.	1.64
Orographic	208.	1.53
Showers	300.	1.37
Showers	200.	1.50
Showers	204.	1.70
Showers	520.	1.81
TRMM	396.	0.82
TRMM	216.	1.44

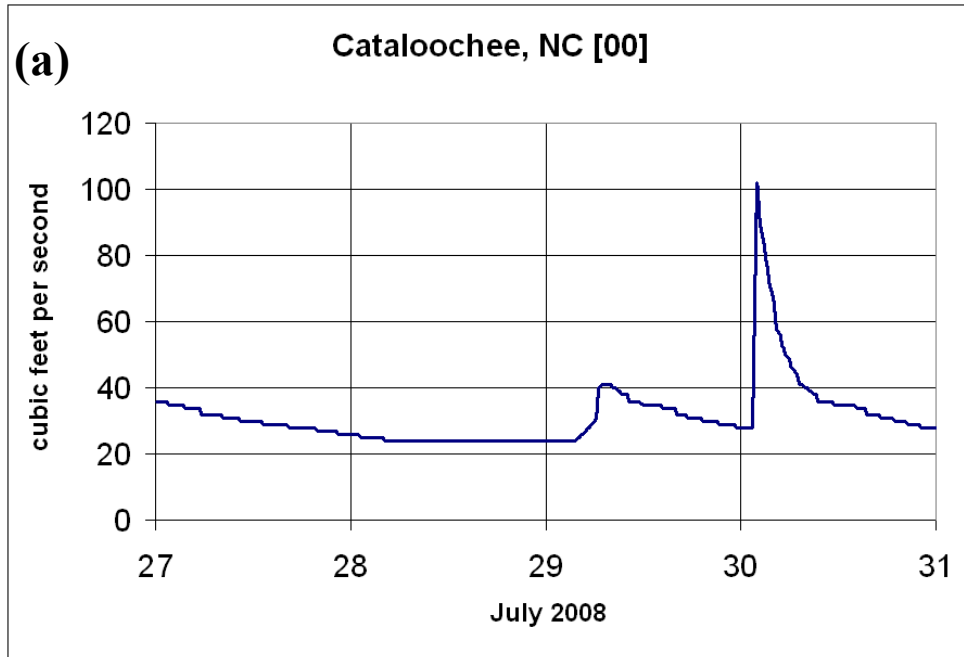
5
6
7
8
9
10
11
12
13
14
15
16
17



1
2

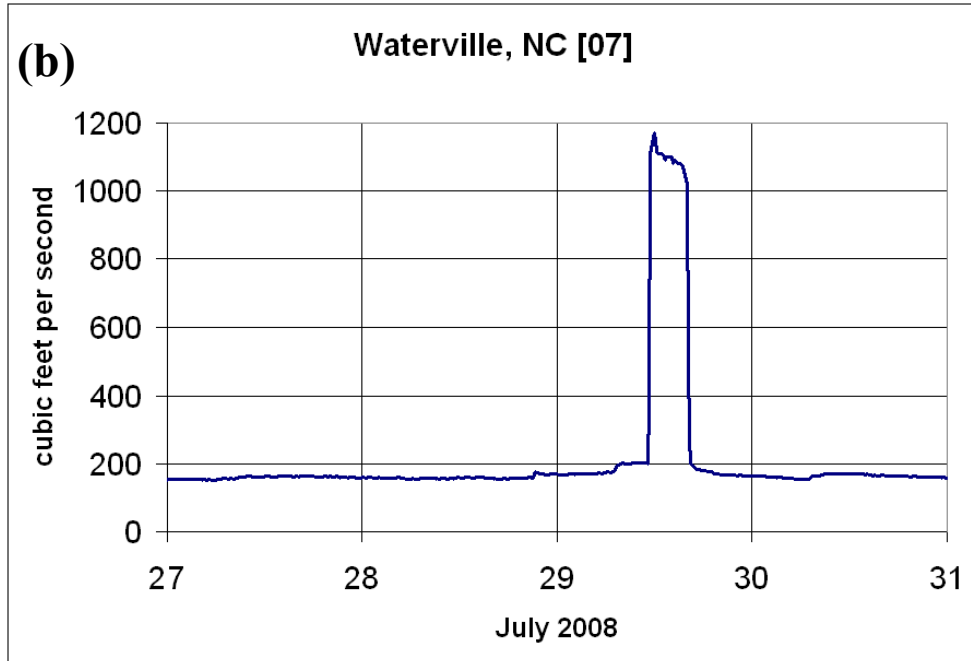
3 Figure 1. Study region within the southern Appalachian Mountains. Haywood County,
 4 NC border is outlined in red. Locations of the KMRX and KGSP NEXRAD stations are
 5 indicated by a red dot. Inset shows borders of the Pigeon River Watershed with rain (star)
 6 and stream (dot) gauge locations highlighted. Gauges #111, #100, and #106 are
 7 highlighted with a square, a circle, and a triangle, respectively. Gauge #100 is located
 8 along the Cataloochee Divide. The stream gauge near Cataloochee, NC, Waterville, NC,
 9 and Newport, TN is labeled '00', '07', and '15', respectively.

10
11
12
13
14
15
16
17



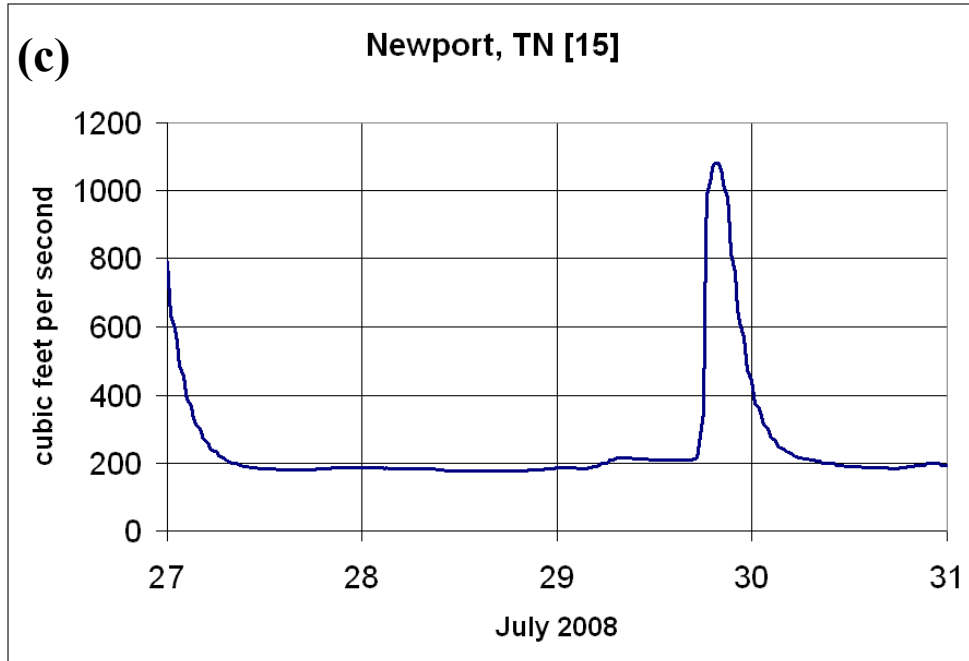
1
2
3
4
5
6
7
8
9
10
11
12
13
14
15
16
17
18

Figure 2. Instantaneous discharge (ft³ s⁻¹) for the USGS river gauges near (a) Cataloochee, NC (#034600000), (b) Waterville, NC (#03460795), and (c) Newport, TN (#03461500) over the period 27 JULY through 30 JUL 2008.



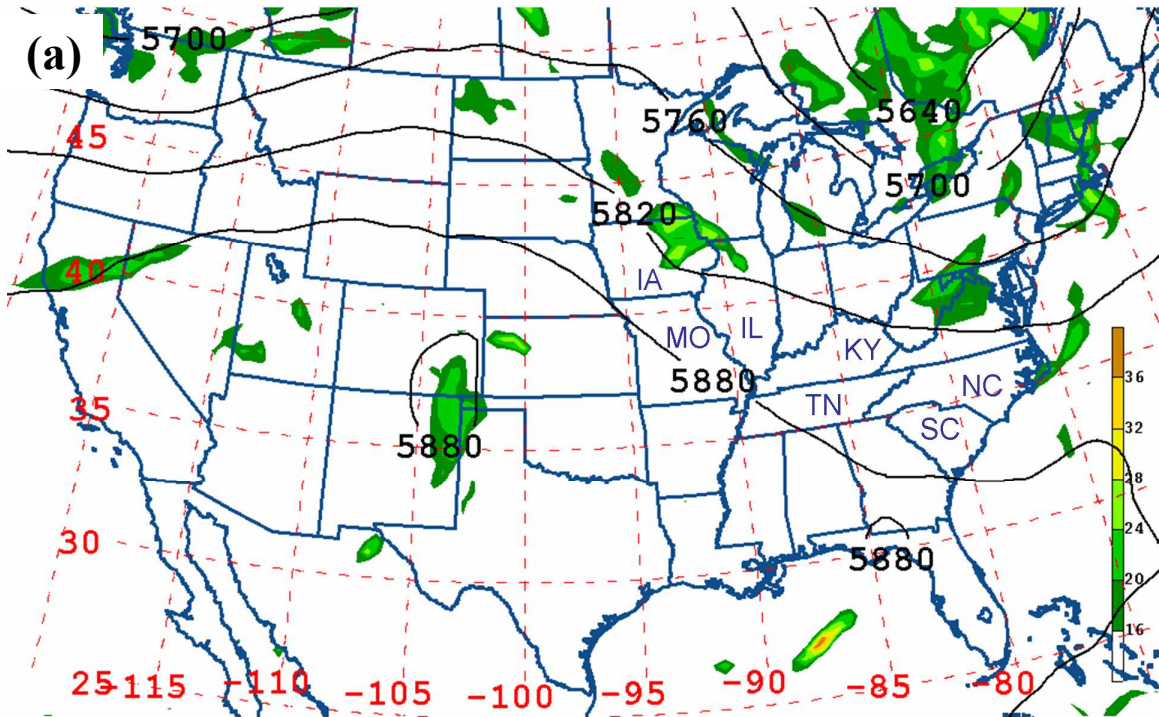
1
2
3
4
5
6
7
8
9
10
11
12
13
14
15
16
17

Fig. 2 (cont.)



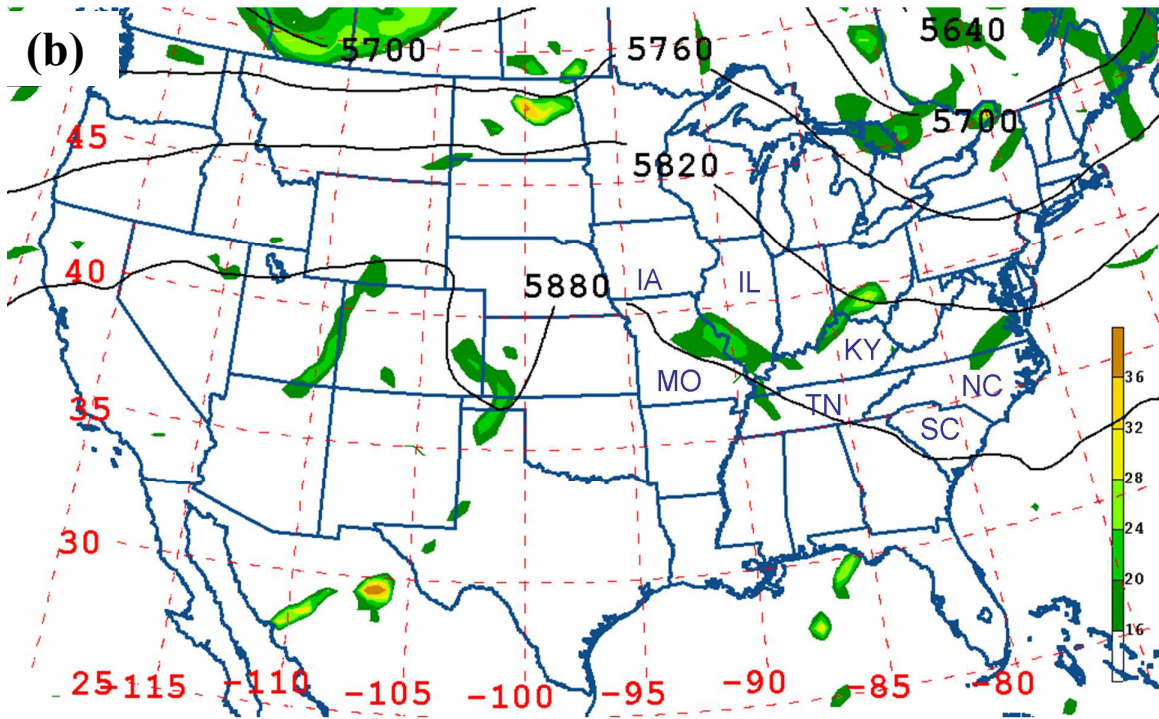
1
2
3
4
5
6
7
8
9
10
11
12
13
14

Fig. 2 (cont.)



1
 2
 3
 4
 5
 6
 7
 8
 9
 10
 11
 12
 13
 14
 15

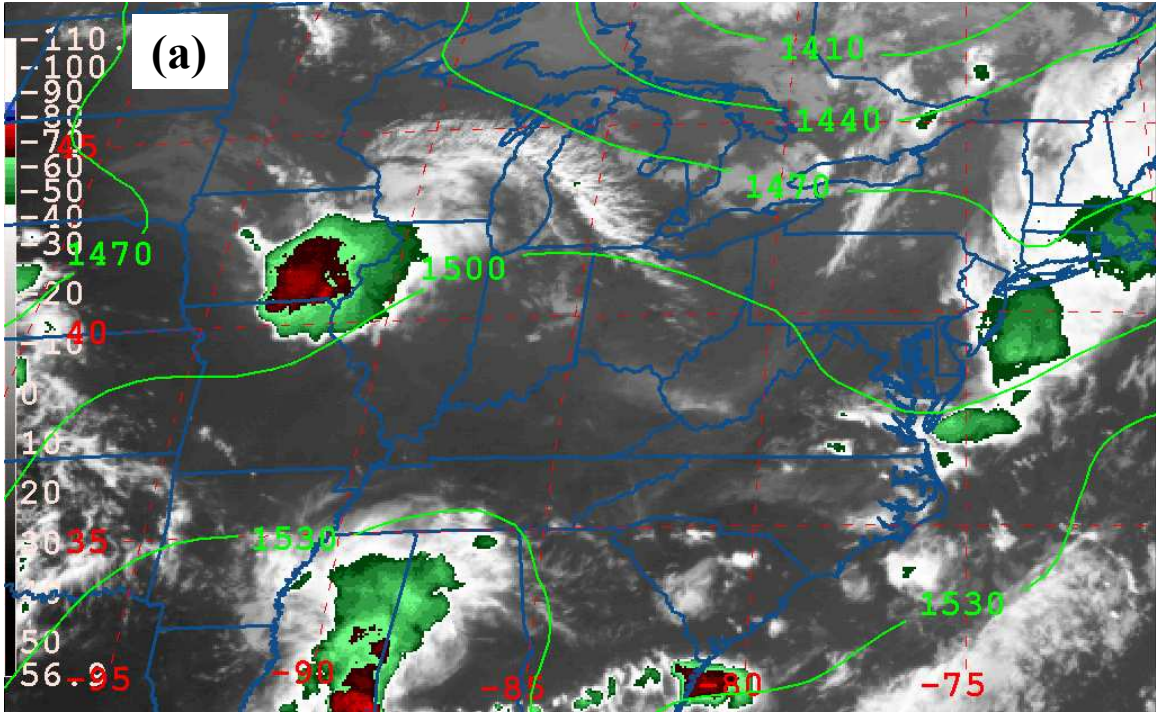
Figure 3. Geopotential height (contours, interval = 60 m) and absolute vorticity (shading, $\times 10^{-5} \text{ s}^{-1}$) at the 500 hPa level derived from NCEP-EDAS valid (a) 0000 UTC and (b) 1800 UTC 28 July 2008.



1
2

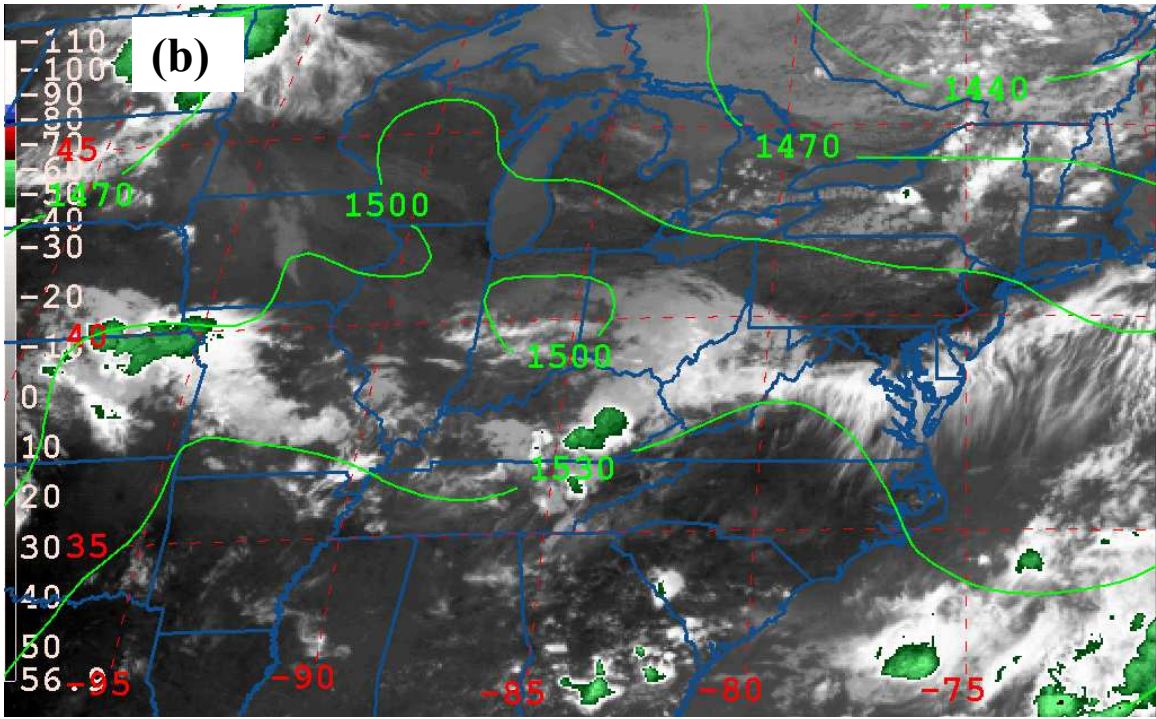
3 Fig. 3 (cont.)

4
5
6
7
8
9
10
11
12
13
14
15
16
17
18
19
20
21
22
23
24
25
26



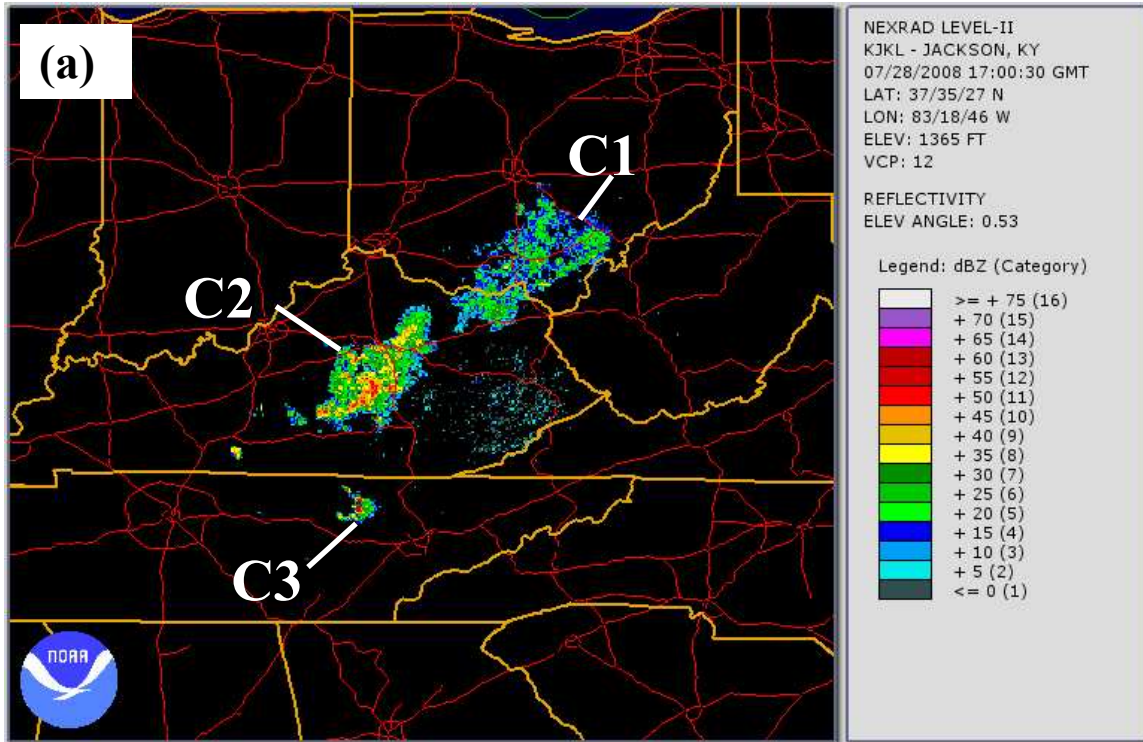
1
2
3
4
5
6
7
8
9
10
11

Figure 4. Geopotential height (contours, interval = 30 m) at the 850 hPa level derived from NCEP-EDAS overlaid with GOES-12 IR brightness temperatures ($^{\circ}\text{C}$) valid (a) 0000 UTC and (b) 1800 UTC 28 July 2008.



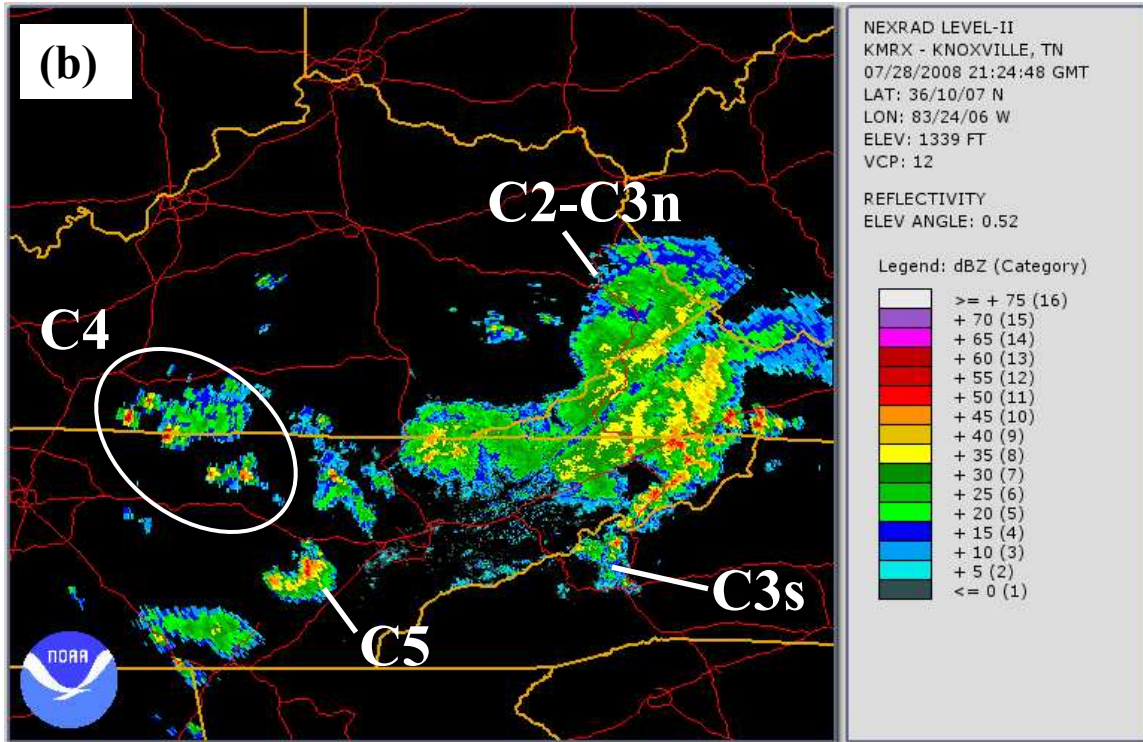
1
2
3
4
5
6
7
8
9
10
11
12
13
14
15
16
17
18
19

Fig. 4 (cont.)



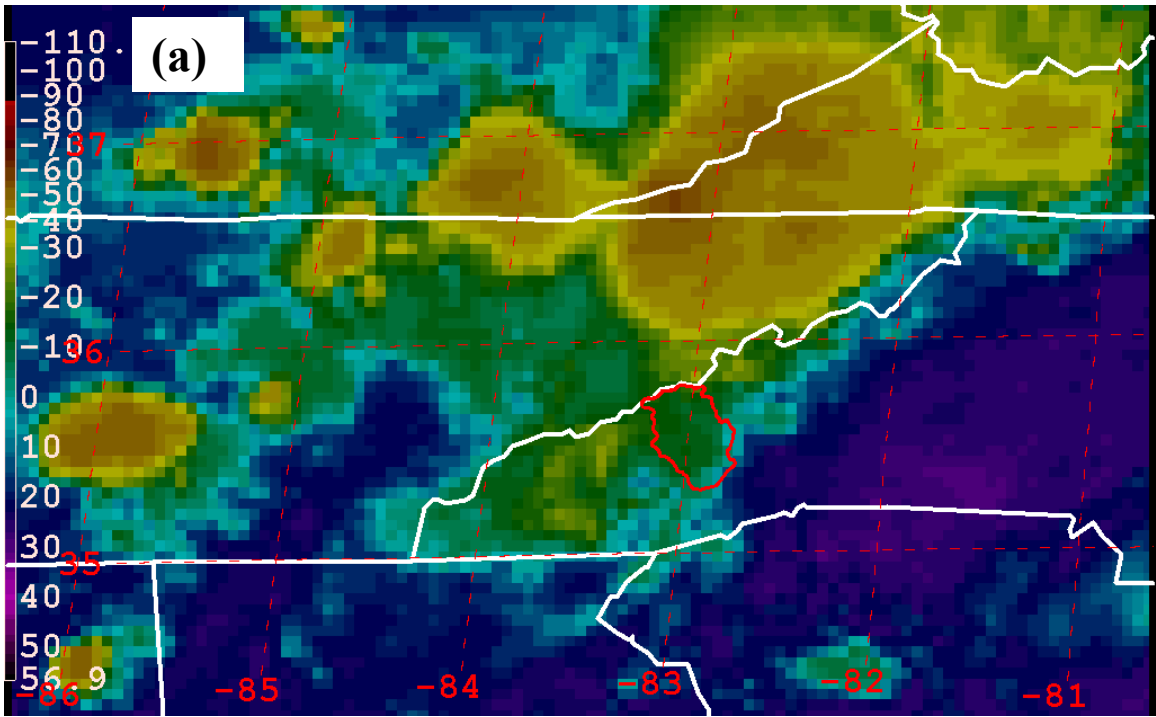
1
 2
 3
 4
 5
 6
 7
 8
 9

Figure 5. NEXRAD base reflectivity (dBZ) at (a) KJKL valid 1700 UTC 28 July 2008 and (b) KMRX valid 2124 UTC 28 July 2008 (images courtesy NCDC).



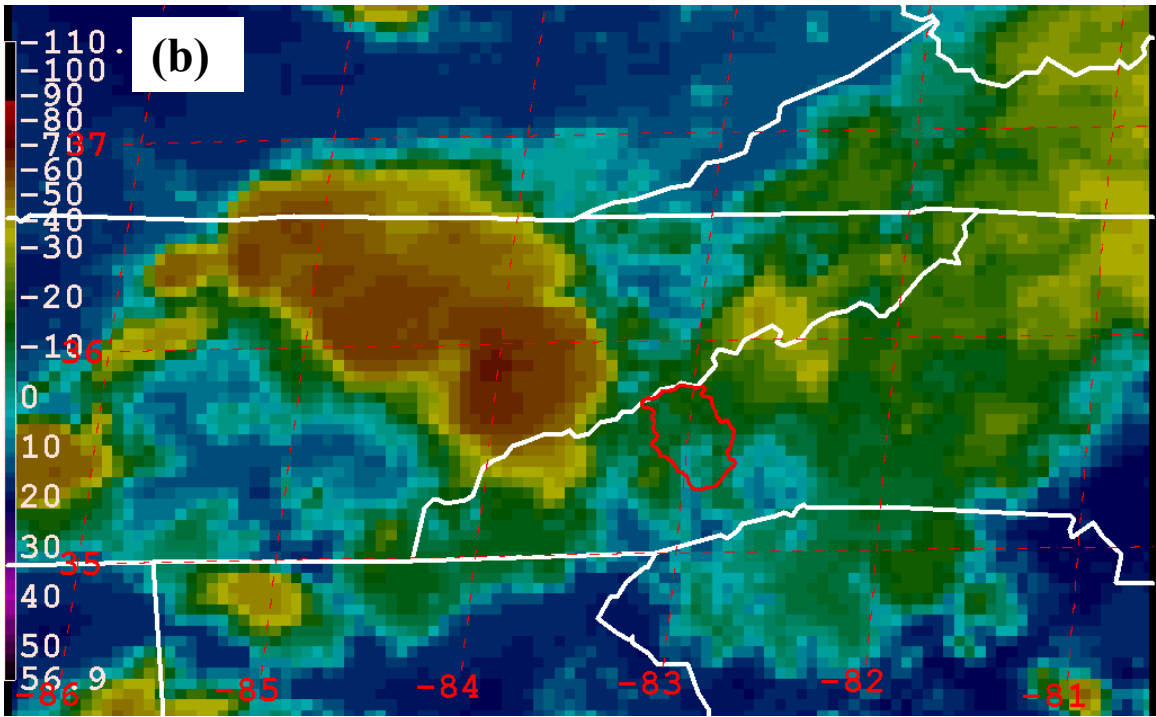
1
 2
 3
 4
 5
 6
 7
 8
 9
 10
 11
 12
 13

Fig. 5 (cont.)



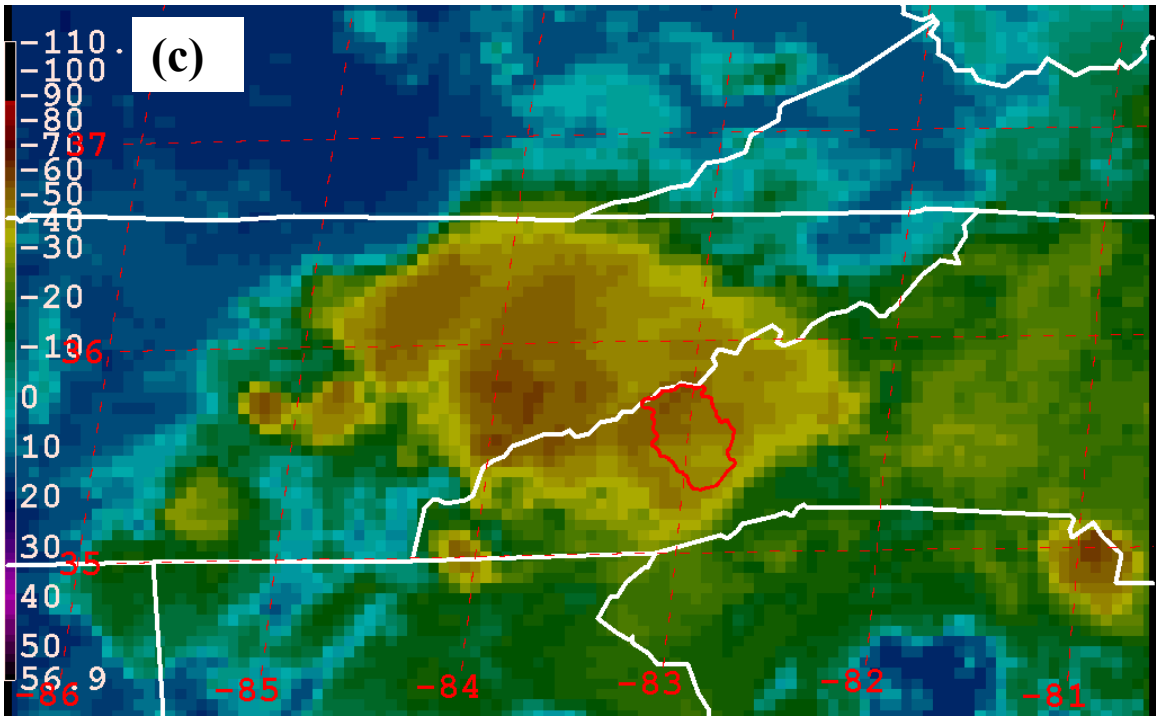
1
2
3
4
5
6
7
8
9
10
11
12

Figure 6. GOES-12 IR brightness temperatures ($^{\circ}\text{C}$) valid (a) 2045 UTC 28 July 2008, (b) 2345 UTC 28 July 2008, (c) 0145 UTC 29 July 2008, and (d) 0415 UTC 29 July 2008. Haywood County, NC is outlined in red.



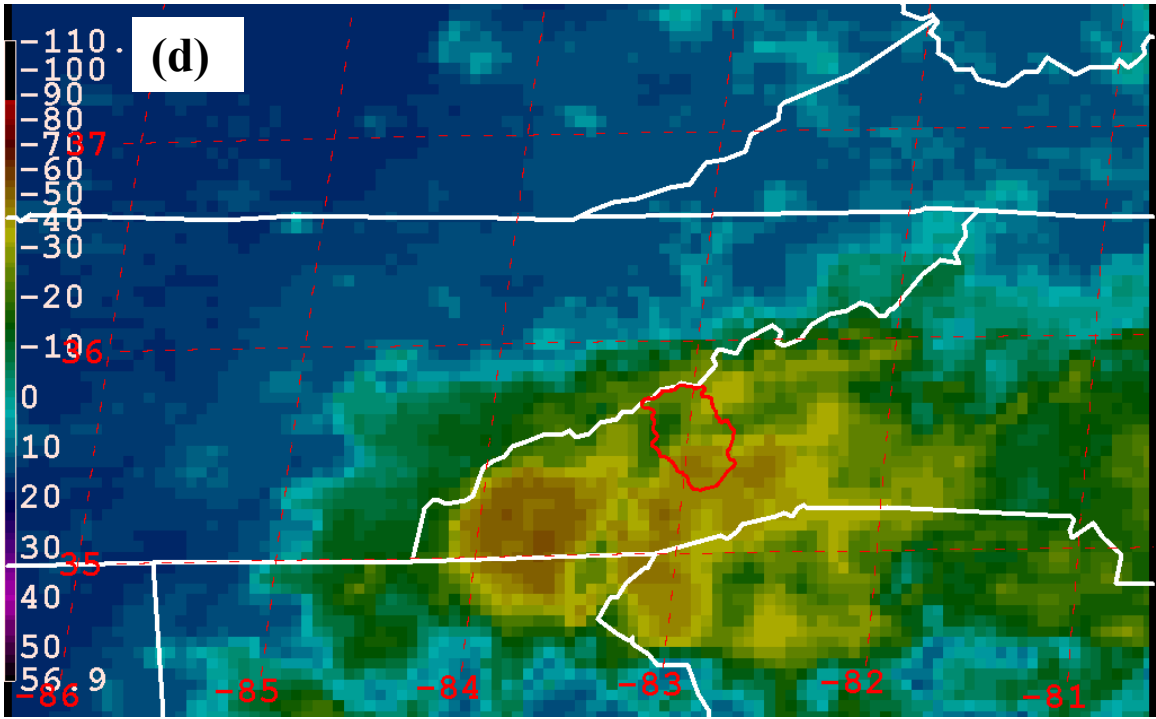
1
2
3
4
5
6
7
8
9
10
11

Fig. 6 (cont.)



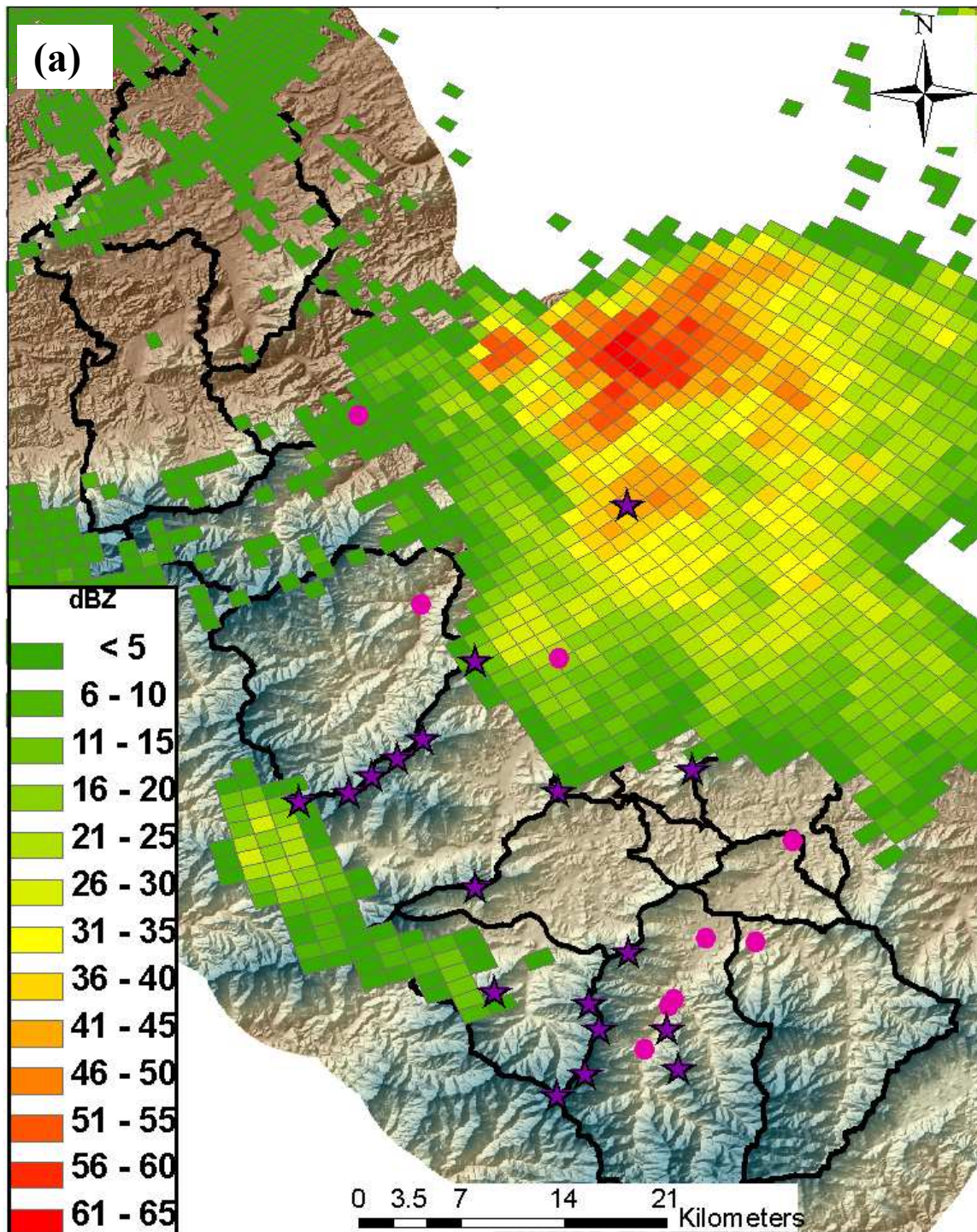
1
2
3
4
5
6
7
8
9
10
11

Fig. 6 (cont.)

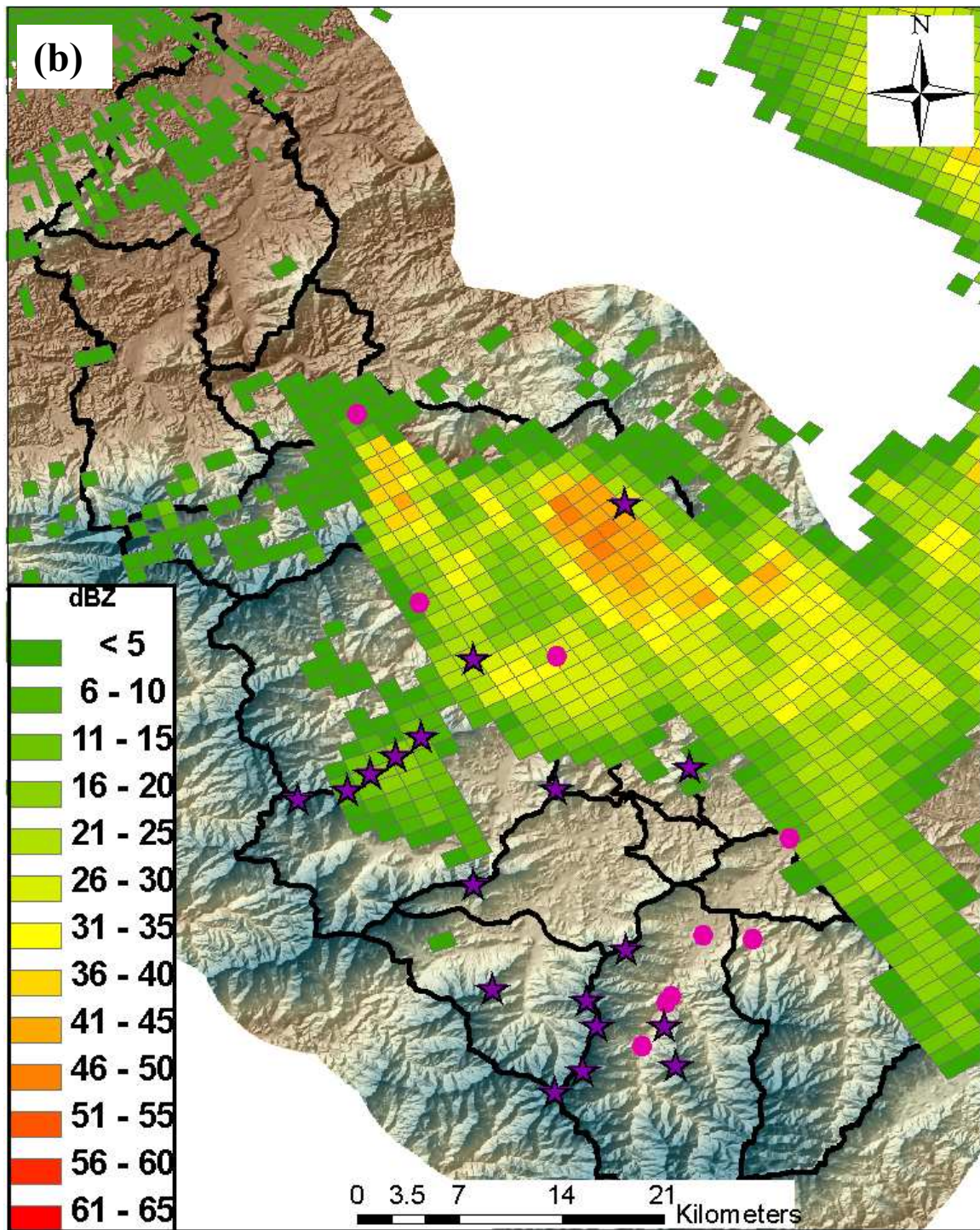


1
2
3
4
5
6

Fig. 6 (cont.)

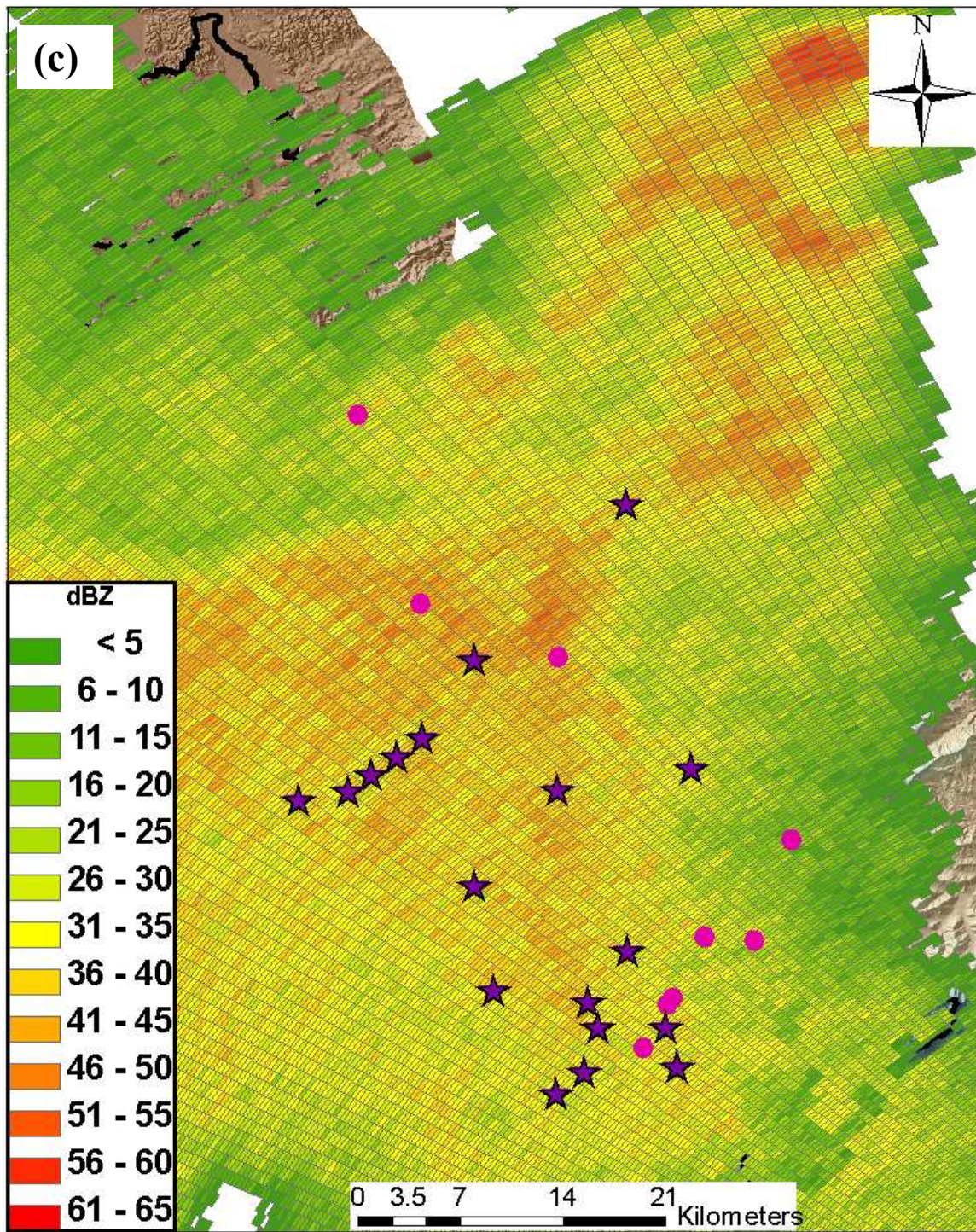


1
 2
 3 Figure 7. NEXRAD reflectivity (dBZ) at (a) KMRX (elevation angle=2.44°) valid 2055
 4 UTC 28 July 2008, (b) KMRX (elevation angle=2.44°) valid 2349 UTC 28 July 2008, (c)
 5 KGSP (elevation angle=1.37°) valid 0155 UTC 29 July 2008, and (d) KGSP (elevation
 6 angle=1.37°) valid 0401 UTC 29 July 2008 for the Pigeon River Watershed with rain
 7 (star) and stream (dot) gauge locations highlighted.



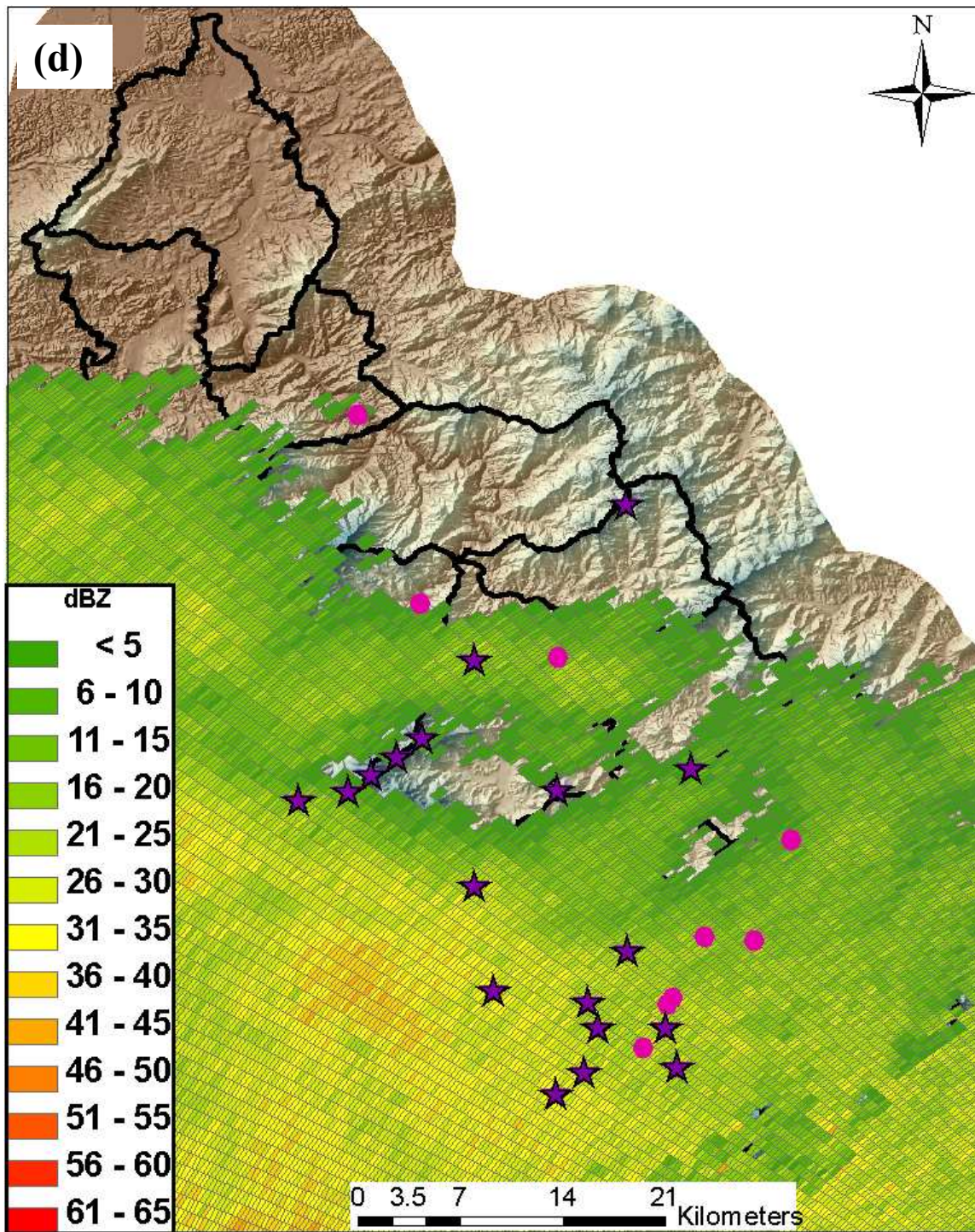
1
2
3
4
5
6

Fig. 7 (cont.)



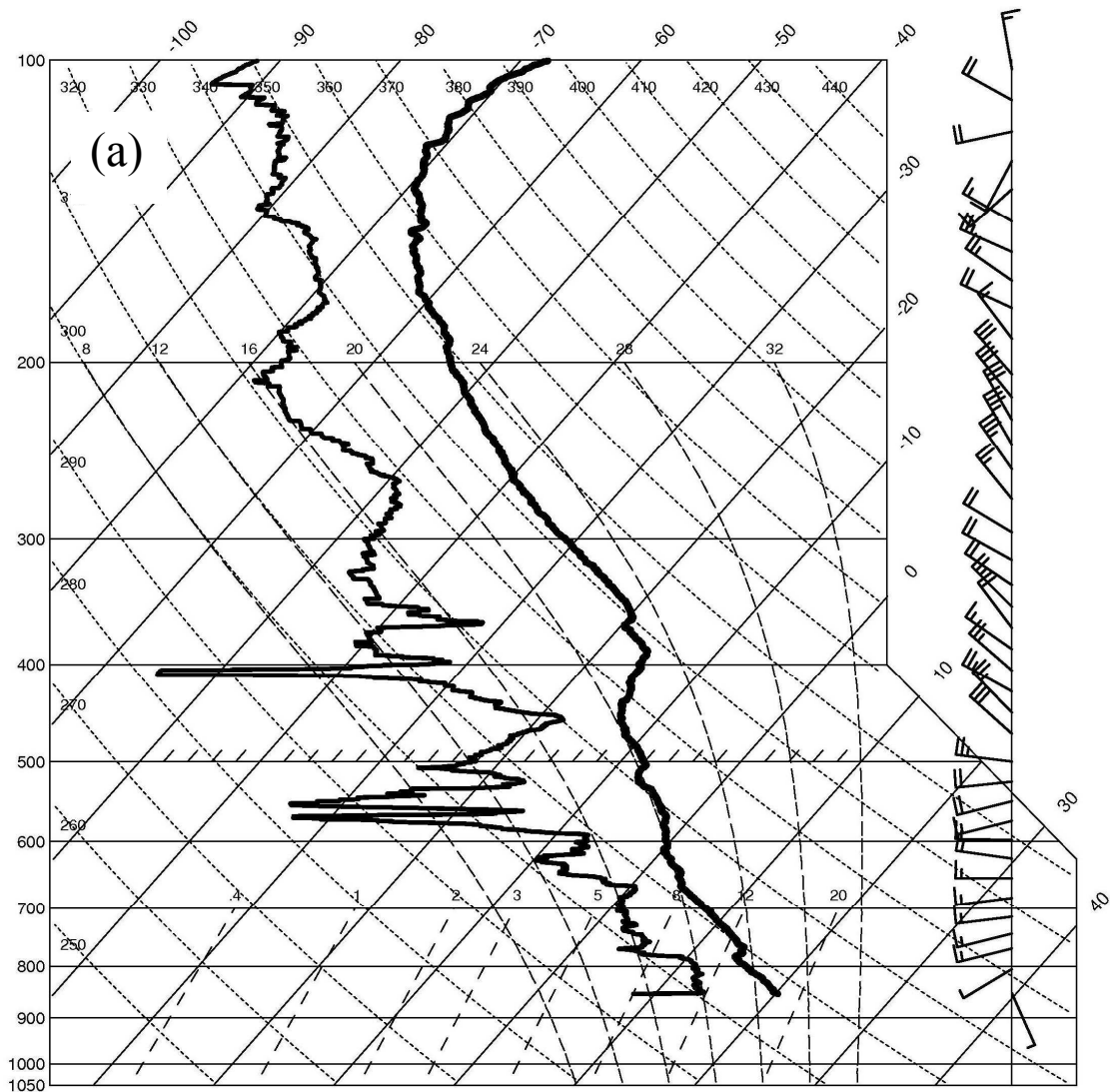
1
2
3
4
5
6

Fig. 7 (cont.)



1
2
3
4
5
6

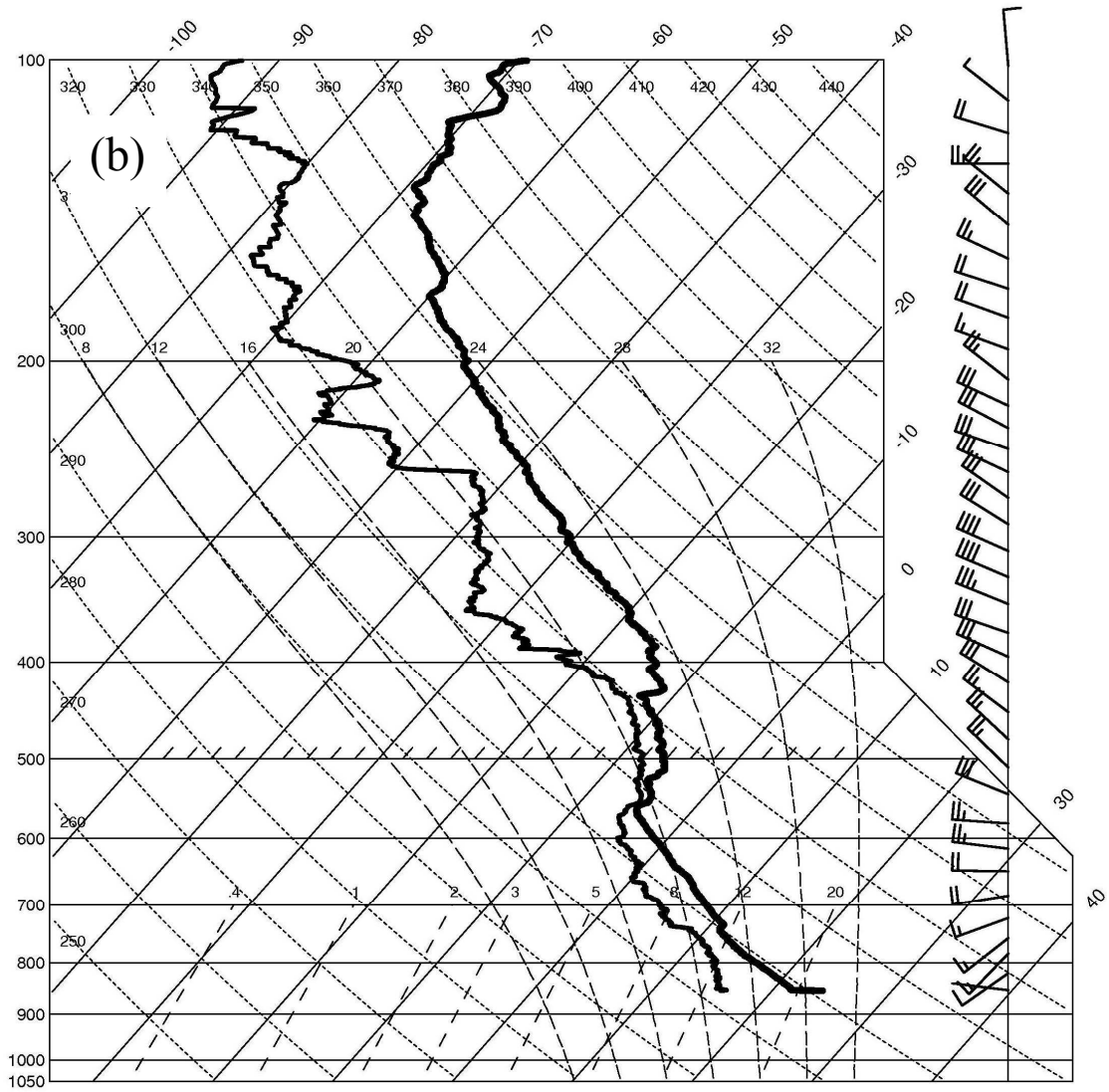
Fig. 7 (cont.)



2008072815 Purchase Knob (35.5859N, 83.0729W) sounding (elv=1495 meters)

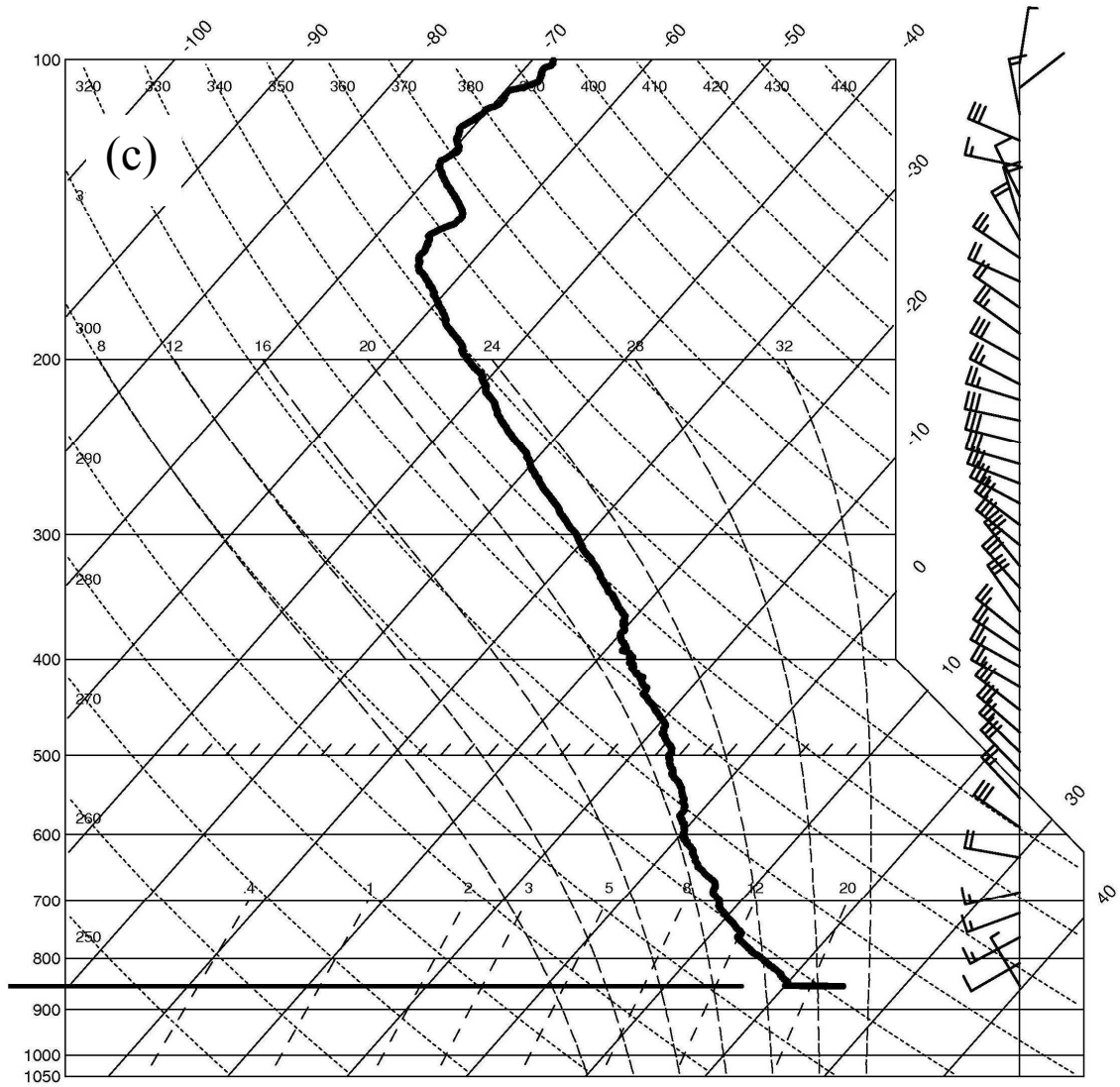
1
2
3
4
5
6

Figure 8. Purchase Knob Skew T – Log P soundings valid (a) 1500 UTC 28 July 2008, (b) 2100 UTC 28 July 2008, (c) 0000 UTC 29 July 2008, and (d) 0300 UTC 29 July 2008.



1
2
3
4

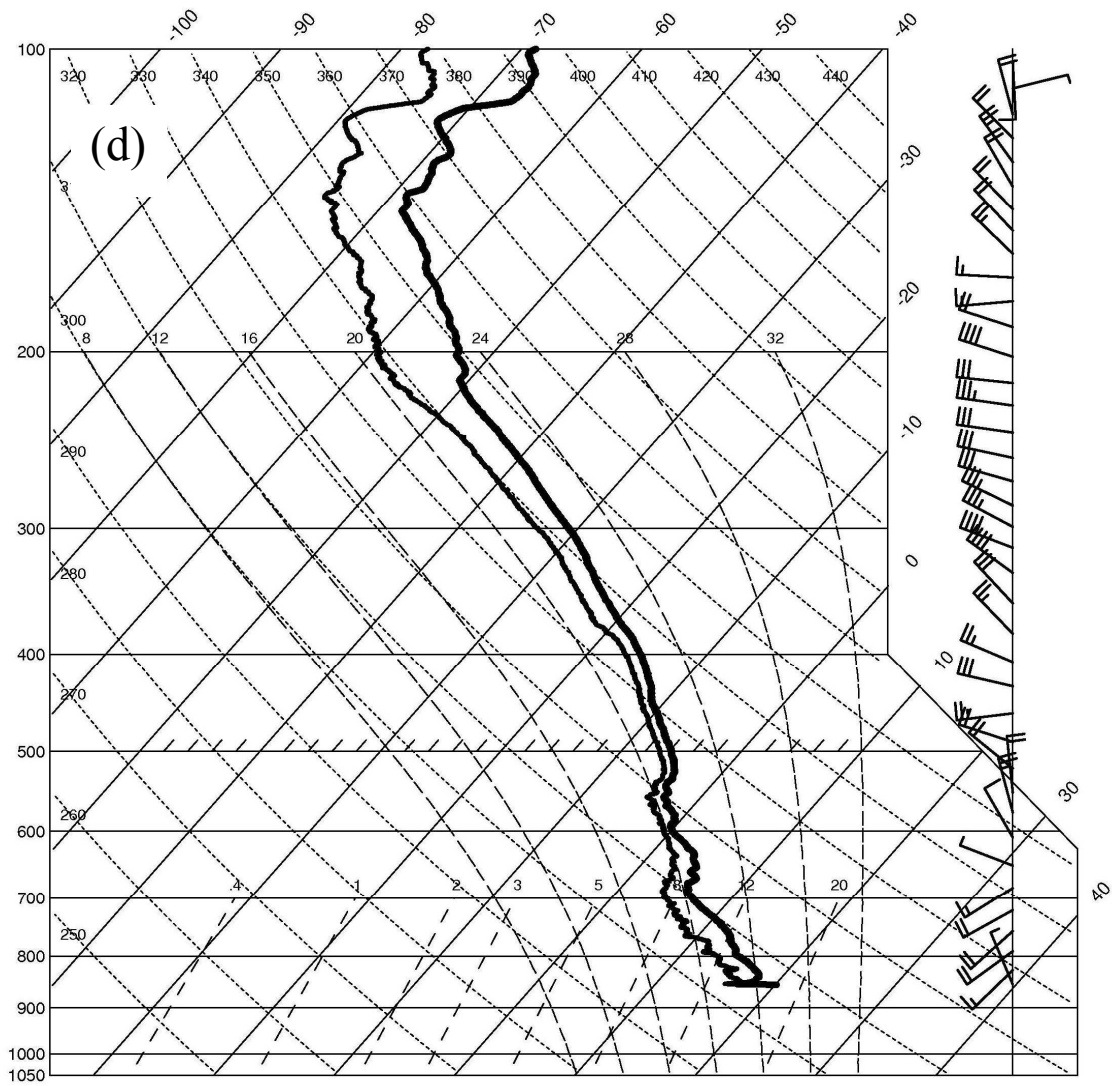
Fig. 8 (cont.)



2008072800 Purchase Knob (35.5859N, 83.0729W) sounding (elv=1495 meters)

- 1
- 2
- 3
- 4

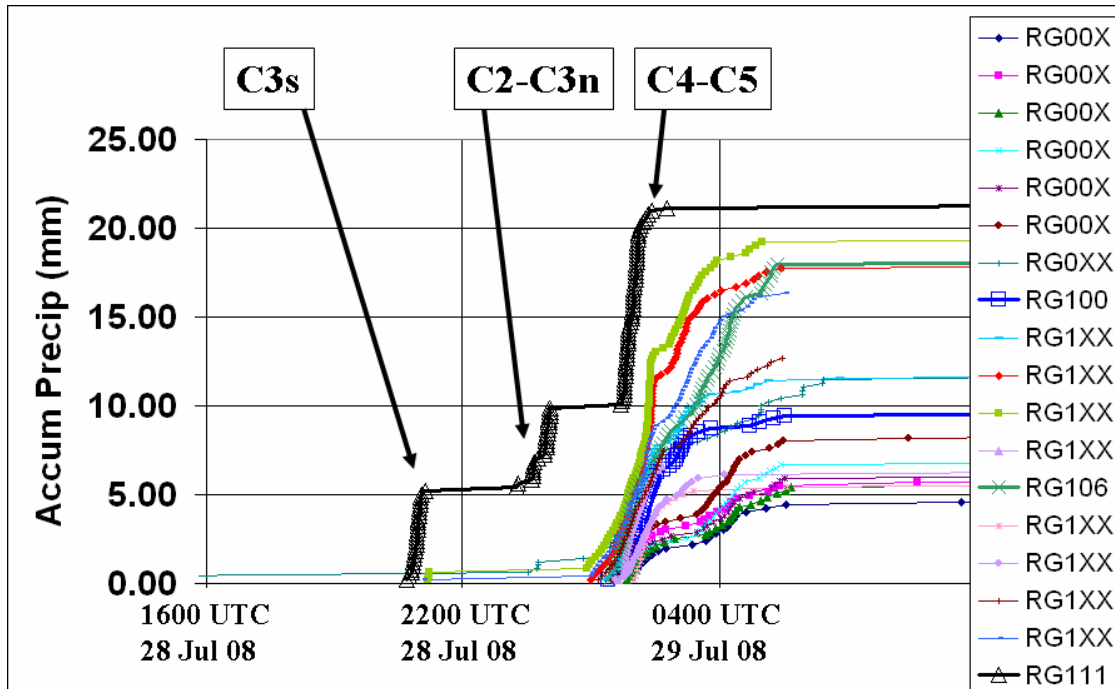
Fig. 8 (cont.)



2008072903 Purchase Knob (35.5859N, 83.0729W) sounding (elv=1495 meters)

1
2
3
4

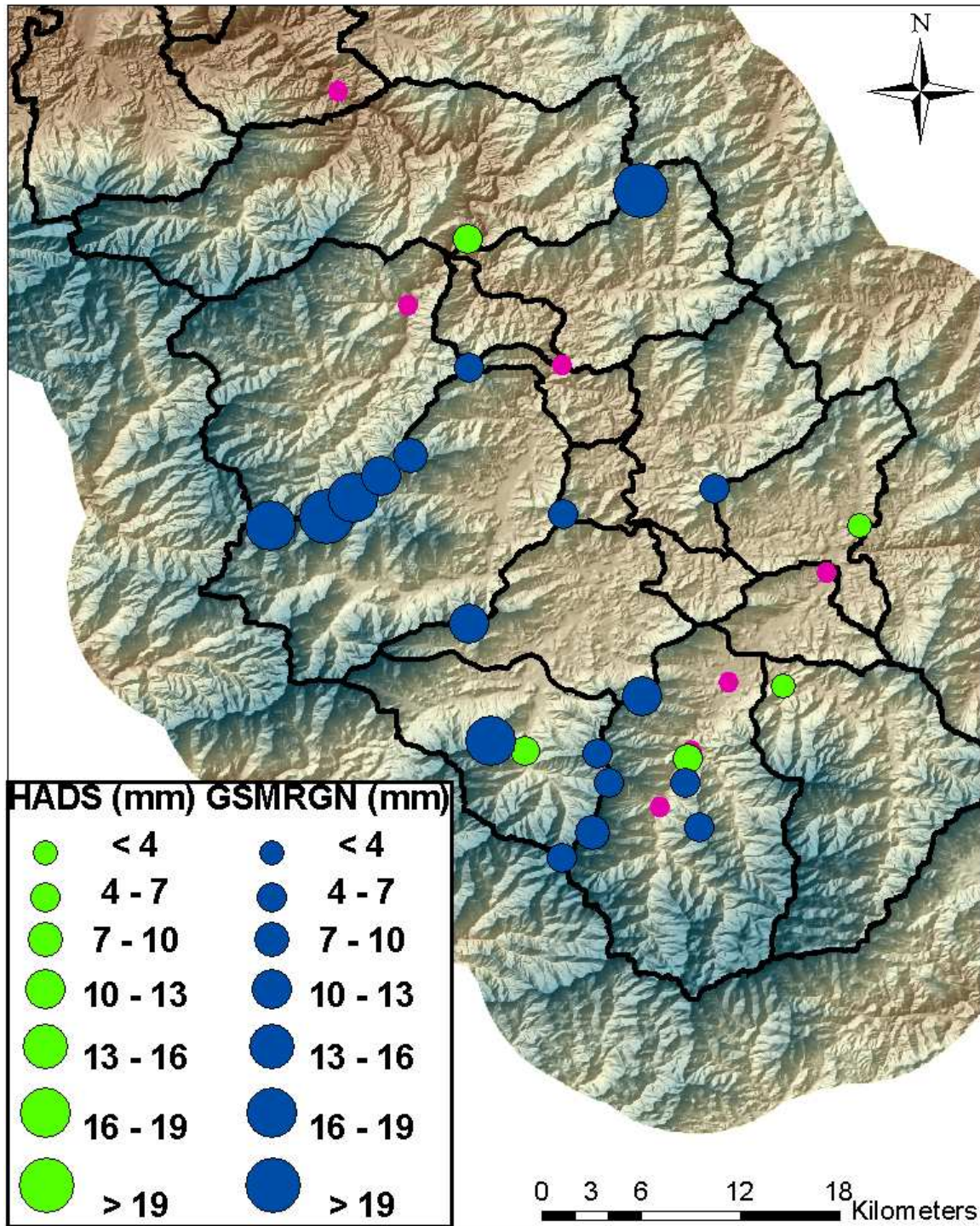
Fig. 8 (cont.)



1
2

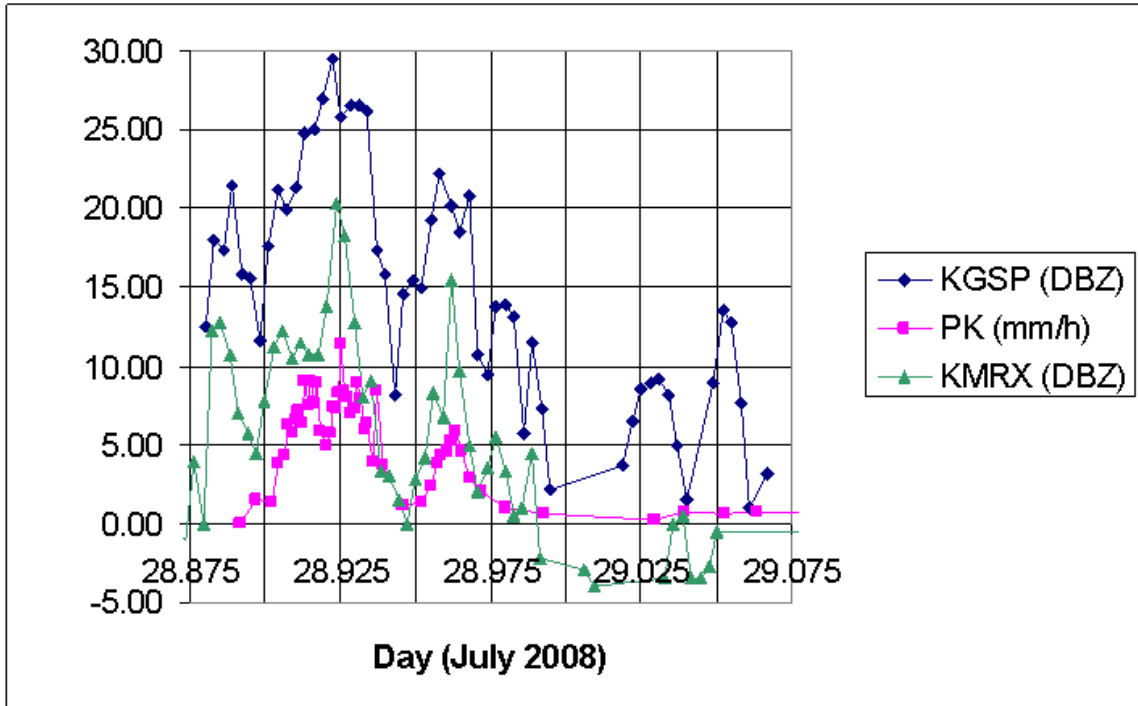
3 Figure 9. Accumulated precipitation (mm) as observed by the Great Smoky Mountain
 4 Rain Gauge Network located in the Pigeon River Watershed over the period 1600 UTC
 5 28 July through 1000 UTC 29 July 2008. Convection responsible for the observed
 6 precipitation at Gauge #111 is labeled.

7
8
9
10
11
12
13
14
15
16
17
18



1
2

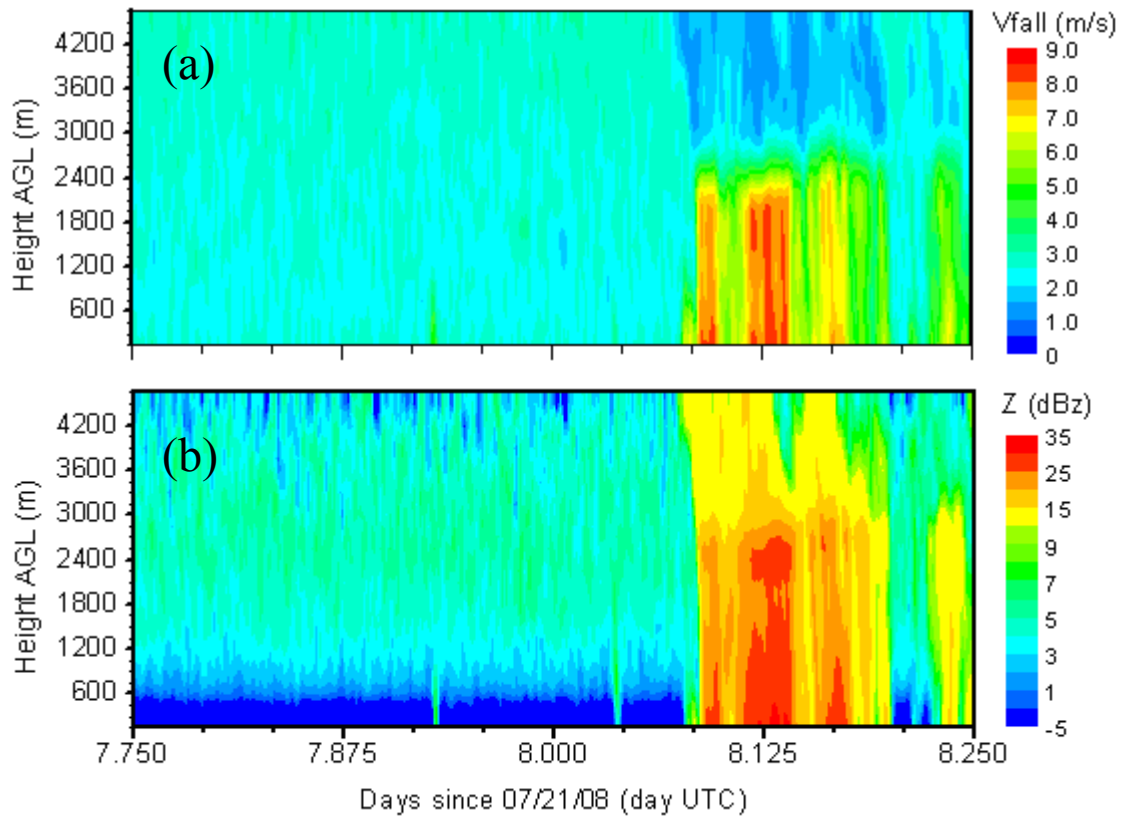
3 Figure 10. Total rainfall (mm) for the period 2100 UTC 28 July through 0600 UTC 29
4 July 2008. Dark blue circles are accumulations for the GSMRGN and green circles are
5 local operational TVA- and USGS-operated rain gauges.



1
2

3 Figure 11. Rain rate (mm h^{-1}) as observed by the Great Smoky Mountain Rain Gauge
 4 Network gauge #100 (squares) located at Purchase Knob in the Pigeon River Watershed
 5 and base reflectivity (dBZ) observed from the KGSP (diamonds, elevation angle= 1.37°)
 6 and KMRX (triangles, elevation angle= 2.44°) NEXRAD sites over the period 0100 UTC
 7 through 0548 UTC 29 July 2008.

8
9
10
11
12
13
14
15
16
17

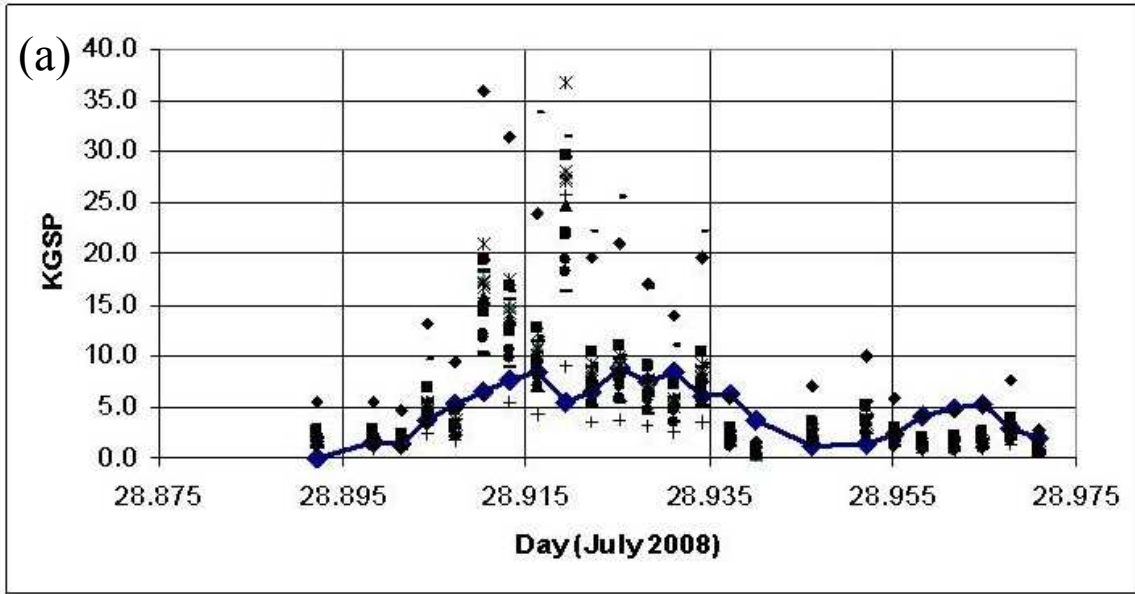


1

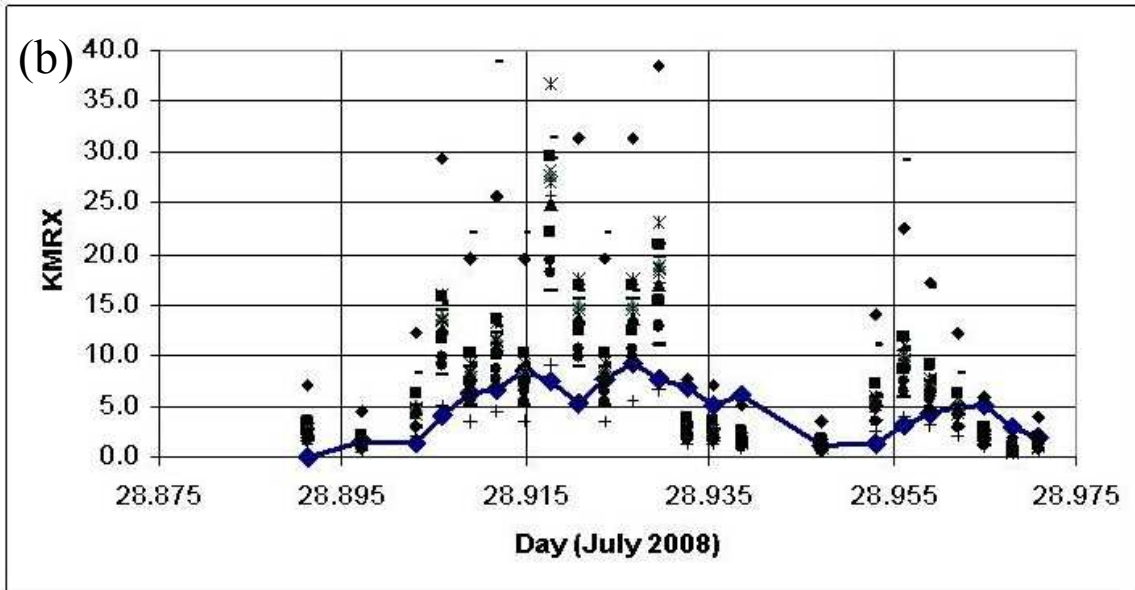
2
3

4 Figure 12. MRR-derived (a) fall velocity (m s^{-1}) and (b) reflectivity (dBZ) at Purchase
5 Knob over the period 1800 UTC 28 July through 0600 UTC 29 July 2008.

6
7
8
9
10
11
12
13
14
15
16
17
18
19



1



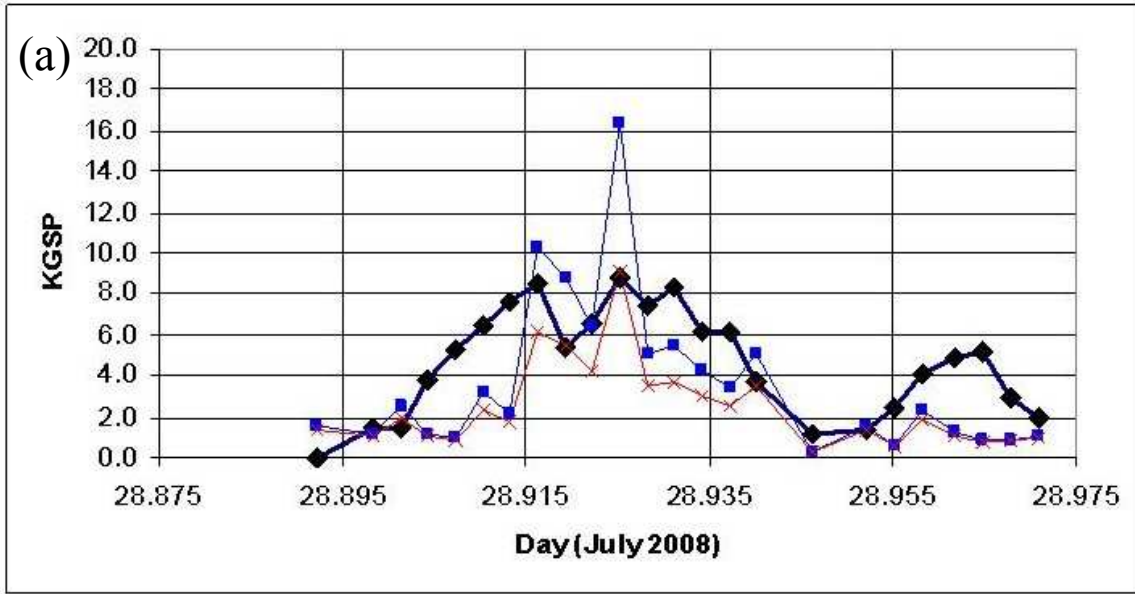
2

3

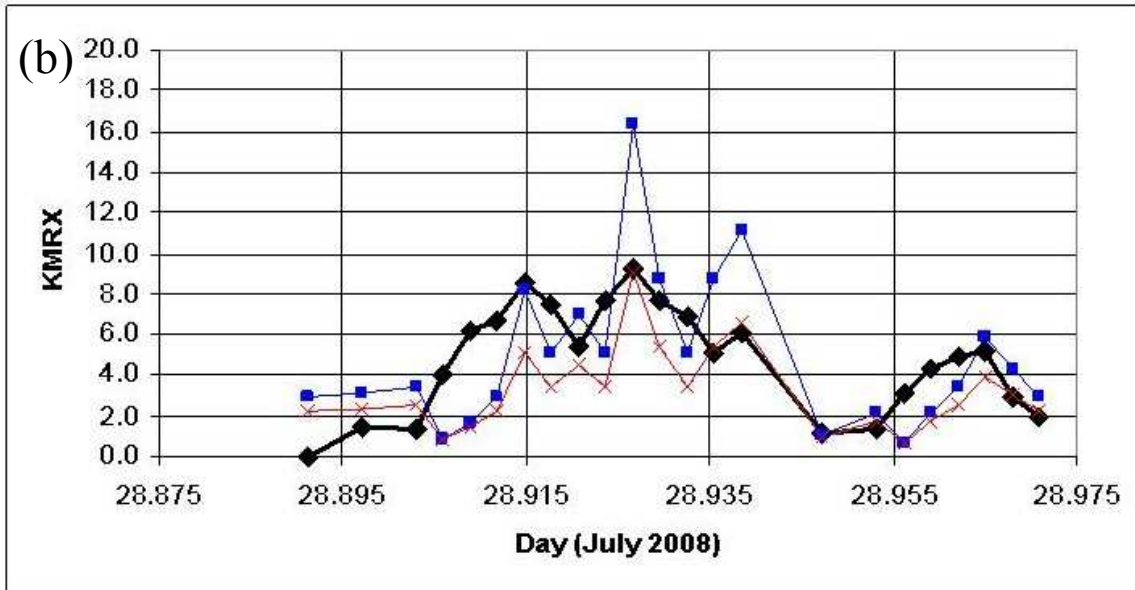
4 Figure 13. Rain rate (mm h^{-1}) as observed by the Great Smoky Mountain Rain Gauge
 5 Network gauge #100 (solid line) located at Purchase Knob in the Pigeon River Watershed
 6 and estimated rain rate (mm h^{-1}) based on 17 Z-R relationships defined in Prat and Barros
 7 (2009) for reflectivity (dBz) observed from the (a) KGSP (elevation angle= 1.37°) and (b)
 8 KMRX (elevation angle= 2.44°) NEXRAD sites over the period 0100 UTC through 0324
 9 UTC 29 July 2008.

10

11



1



2

3

4 Figure 14. Rain rate (mm h^{-1}) as observed by the Great Smoky Mountain Rain Gauge
 5 Network gauge #100 (thick solid line, diamonds) located at Purchase Knob in the Pigeon
 6 River Watershed and estimated rain rate (mm h^{-1}) based on Z-R relationships for
 7 “Showers” ($A=520$, $b=1.81$, red line) and for “Thunderstorms” ($A=450$, $b=1.48$, blue
 8 line) as defined in Prat and Barros (2009) for reflectivity (dBz) observed from the (a)
 9 KGSP (elevation angle= 1.37°) and (b) KMRX (elevation angle= 2.44°) NEXRAD sites
 10 over the period 0100 UTC through 0324 UTC 29 July 2008.